

In vivo confocal microscopy of the ocular surface: from bench to bedside

Journal:	<i>Current Eye Research</i>
Manuscript ID:	NCER-2013-0202.R1
Manuscript Type:	Mini Review
Date Submitted by the Author:	25-Aug-2013
Complete List of Authors:	Villani, Edoardo; University of Milan, Baudouin, Christophe; Quinze-Vingts National Ophthalmology Hospital, Efron, Nathan; Institute of Health and Biomedical Innovation, and School of Optometry and Vision Science, Queensland University of Technology, Hamrah, Pedram; Massachusetts Eye & Ear Infirmary, Harvard Medical School, Department of Ophthalmology; Kojima, Takashi; Keio University School of Medicine, Department of Ophthalmology Patel, Sanjay; Mayo Clinic, Ophthalmology Pflugfelder, Stephen; Ocular Surface Center, Cullen Eye Institute, Department of Ophthalmology, Baylor College of Medicine, Zhivov, Andrey; University of Rostock, Ophthalmology; Dogru, Murat; Keio University School of Medicine, J&J Ocular Surface and Visual Optics; ; Keio University School of Medicine, Department of Ophthalmology
Keywords:	confocal microscopy , keratitis, dry eye, keratoplasty, glaucoma, contact lens, ocular surface, imaging, cornea, conjunctiva

***In vivo* confocal microscopy of the ocular surface: from bench to bedside**

Edoardo Villani,¹ Christophe Baudouin,² Nathan Efron,³ Pedram Hamrah,⁴ Takashi Kojima,⁵ Sanjay V. Patel,⁶ Stephen C. Pflugfelder,⁷ Andrey Zhivov,⁸ Murat Dogru⁵

1. University of Milan, Department of Clinical Sciences and Community Health. Eye Clinic San Giuseppe Hospital, Milan. Eye Clinic Fondazione IRCCS Ca' Granda Ospedale Maggiore Policlinico of Milan, Italy.

2. Quinze-Vingts National Ophthalmology Hospital, Paris, France.

3. Institute of Health and Biomedical Innovation, and School of Optometry and Vision Science, Queensland University of Technology, Kelvin Grove, Queensland, Australia.

4. Ocular Surface Imaging Center, Cornea & Refractive Surgery Service, Massachusetts Eye and Ear Infirmary, Department of Ophthalmology, Harvard Medical School, Boston, MA, USA.

5. Department of Ophthalmology, Keio University School of Medicine, Tokyo, Japan.

6. Department of Ophthalmology, Mayo Clinic, Rochester, MN, USA.

7. Ocular Surface Center, Cullen Eye Institute, Department of Ophthalmology, Baylor College of Medicine, Houston, TX, USA.

8. Department of Ophthalmology, University of Rostock, Rostock, Germany.

Corresponding authors:

Edoardo Villani (email: edoardo.villani@unimi.it)

Murat Dogru (email: muratodooru2005@yahoo.co.jp)

Abstract

In vivo confocal microscopy (IVCM) is an emerging technology that provides minimally invasive, high resolution, steady-state assessment of the ocular surface at the cellular level. Several challenges still remain but, at present, IVCM may be considered a promising technique for clinical diagnosis and management. This mini-review summarizes some key findings in IVCM of the ocular surface, focusing on recent and promising attempts to move “from bench to bedside”.

IVCM allows prompt diagnosis, disease course follow-up, and management of potentially blinding atypical forms of infectious processes, such as Acanthamoeba and fungal keratitis. This technology has improved our knowledge of corneal alterations and some of the processes that affect the visual outcome after lamellar keratoplasty and excimer keratorefractive surgery. In dry eye disease, IVCM has provided new information on the whole ocular surface morpho-functional unit. It has also improved understanding of pathophysiological mechanisms and helped in the assessment of prognosis and treatment.

IVCM is particularly useful in the study of corneal nerves, enabling description of the morphology, density, and disease- or surgically induced alterations of nerves, particularly the subbasal nerve plexus. In glaucoma, IVCM constitutes an important aid to evaluate filtering blebs, to better understand the conjunctival wound healing process, and to assess corneal changes induced by topical antiglaucoma medications and their preservatives.

IVCM has significantly enhanced our understanding of the ocular response to contact lens wear. It has provided new perspectives at a cellular level on a wide range of contact lens complications, revealing findings that were not previously possible to image in the living human eye.

The final section of this mini-review provides a focus on advances in confocal microscopy imaging. These include 2D wide-field mapping, 3D reconstruction of the cornea, and automated image analysis.

Key words: confocal microscopy, keratitis, dry eye, keratoplasty, glaucoma

1
2
3 In vivo confocal microscopy (IVCM) is a rapidly evolving imaging and diagnostic tool, which
4 offers an exciting bridge between clinical and laboratory observations, enabling clinicians and
5 scientists to gain insight into alterations of the ocular surface microstructure, both in health and
6 disease.⁽¹⁾
7
8

9
10 In contrast to conventional microscopy in which the image can be observed directly (all points in the
11 specimen are imaged parallel), a CM optimizes illumination and detection for a single spot only.⁽²⁾
12

13
14 At present, the most widely used IVCM reported in the published literature are the Confoscan series
15 (NIDEK, Gamagori, Japan) and the HRTII/Rostock Corneal Module (Heidelberg Engineering
16 GmbH, Heidelberg, Germany).⁽¹⁾
17

18
19 The firsts are white light slit scanning confocal microscopes. With this technology many points
20 along the axis of the slit can be scanned in parallel, greatly reducing scanning times and the required
21 intensity of the light source. However, these instruments are only truly confocal in the axis
22 perpendicular to the slit height and provides lower transverse and axial resolution.⁽¹⁾
23

24
25 The HRTII/Rostock Corneal Module is a laser scanning confocal microscope. This instrument uses
26 a coherent high intensity light source and the laser beam is scanned over the back of the microscope
27 objective by a set of galvanometer scanning mirrors.⁽¹⁾ Because of the high-depth resolution, optical
28 sections of only a few micrometers can be imaged and precisely measured in combination with a
29 high contrast.⁽²⁾
30

31
32 Studying the cornea, the Confoscan 4 (the last of the Confoscan series) produces high quality
33 images throughout the depth of the cornea with accurate depth information.⁽³⁾ In comparison, the
34 HRT III/RCM produces very detailed images of the anterior cornea but is less accurate in
35 determining depth or producing high quality images of the posterior cornea. The ability of the laser
36 IVCM to examine the different components of the ocular surface has opened new lanes for studying
37 the physiology and pathology of this complex morpho-functional unit.
38

39
40 This mini-review does not provide an exhaustive review of the literature but rather summarizes
41 some key findings in IVCM of the ocular surface, focusing on recent and promising attempts to
42 move “from bench to bedside”. The role of IVCM in the management of infectious keratitis, corneal
43 transplantation, refractive surgery, dry eye disease, and imaging of corneal nerves, assessment of
44 the ocular surface in glaucomatous patients and contact lens wearers are the main topics of this
45 review. The final section provides a focus on advances in confocal microscopy imaging.
46

47
48 ***In Vivo Confocal Microscopy in Management of Infectious Keratitis***
49
50
51
52
53
54
55
56
57
58
59
60

1
2
3 Infectious keratitis is a common condition that can lead to sight-threatening complications and
4 blindness.⁽⁴⁾ Early and accurate diagnosis, as well as subsequent initiation of appropriate therapy
5 have been demonstrated to be the key in prevention of permanent vision loss.⁽⁴⁾ Although clinically,
6 patient history and slit-lamp examination are essential in raising suspicion for the underlying
7 etiology, microbiology remains the gold standard. However, the high false-negative rate and delay
8 of corneal cultures due to slow-growing organisms such as fungi and Acanthamoeba are important
9 limitations to their diagnostic ability.⁽⁵⁾ Given the importance of timing in diagnosis and initiation of
10 therapy, there is an exciting emerging role for IVCN evolving not only for the diagnosis, but also
11 potentially in the management of this disease.⁽⁶⁾

12 Acanthamoeba Keratitis

13 Acanthamoeba is a protozoan that is ubiquitously found in soil, water and air. While the infection
14 rate was reported to be 1.2 per million adults and 0.2-1 per 10,000 contact lens wearers per year,⁽⁷⁾
15 rates have recently risen to more than seven-fold in contact lens wearers.⁽⁸⁾ Acanthamoeba keratitis
16 is often misdiagnosed due to initially nonspecific presentation. The typical ring infiltrate and radial
17 perineuritis may develop at later stages and raise suspicion, at which time the prognosis is guarded
18 and cases require surgical intervention.⁽⁹⁾ Therefore, there is great value in more rapid identification
19 of the organism. Unfortunately, cultures can take weeks to become positive and sensitivity ranges
20 from 0 to 68%.⁽⁹⁾ Further, although polymerase chain reaction (PCR) diagnosis has a better
21 sensitivity for more superficial cases,⁽¹⁰⁾ it is costly, needs technical expertise and is not yet
22 available in all laboratories. **The pharmacotherapy for Acanthamoeba keratitis is expensive,
23 prolonged, and toxic and toxicity may become difficult to distinguish from persistent infection.
24 IVCN may thus be helpful in determination of therapeutic efficacy and persistence or absence of
25 Acanthamoeba noninvasively, potentially improving patient outcomes and decrease the need for
26 surgical intervention.**⁽¹¹⁾

27 Acanthamoeba presents as active trophozoites and/or quiescent cysts, with both forms being
28 identifiable on IVCN, allowing for rapid, same-day diagnosis. Detection of Acanthamoeba by
29 IVCN was first reported in 1992⁽¹²⁾ and was recently supported by The American Academy of
30 Ophthalmology as an adjunctive diagnostic modality.⁽¹³⁾ Double-walled cysts appear as hyper-
31 reflective, spherical, occasionally ovoid, structures, ranging 15-28 micrometers in diameter (Fig. 1
32 A, B). The double-wall may not always be apparent by IVCN, making it occasionally difficult to
33 differentiate cysts from leukocyte or epithelial nuclei. Clustering (Fig. 1A) and rows (Fig. 1B) of
34 cysts are typically suggestive of active proliferative disease. Trophozoites are 25-40 micrometers in
35
36
37
38
39
40
41
42
43
44
45
46
47
48
49
50
51
52
53
54
55
56
57
58
59
60

1
2
3 diameter,⁽⁷⁾ and appear as hyper-reflective and ovoid structures on IVCM (Fig. 1 C, D) but are
4
5 difficult to distinguish from leukocytes and keratocyte nuclei.

6
7 Several single-observer studies have demonstrated a sensitivity of 90.9-100%, and a specificity of
8
9 77.3-100% by IVCM.⁽¹⁴⁻¹⁶⁾ Another study, studying grading by different observers with variable or
10
11 no experience, demonstrated a sensitivity of up to 55.8% and specificity up to 84.2%,⁽¹⁷⁾ underlining
12
13 the importance of training and experience in evaluation of IVCM images.

14 Fungal Keratitis

15
16 The clinical presentation of fungal keratitis is nonspecific and indolent, resulting in delayed therapy
17
18 and potential development into endophthalmitis and loss of the eye. Alternatively, the permanent
19
20 scarring associated with the delay in treatment can lead to significant vision loss. The gold standard
21
22 for diagnosis are corneal smear and cultures, both of which have a limited sensitivity and cultures
23
24 can take several days to weeks to obtain growth.

25 **IVCM is a tool for identification of both filamentous fungi and yeast.** Aspergillus hyphae are hyper-
26
27 reflective 5-10 micrometers in diameter and have septate hyphae with dichotomous branches at a 45
28
29 degree angle (Fig. 2A).⁽⁶⁾ In contrast, Fusarium typically branches at a 90 degree angle.⁽⁸⁾
30
31 Paecilomyces have variable branching and demonstrate loops on IVCM as well (Fig. 2B).⁽¹⁸⁾ The
32
33 hyper-reflective elements seen on IVCM must be differentiated from subbasal corneal nerves,
34
35 which have a more regular branching pattern, as well as from stromal nerves that are much larger in
36
37 diameter (25-50 micrometers). Filamentous fungi are 200-400 micrometers long. In addition, yeast
38
39 such as Candida Albicans, have round, budding bodies that may develop pseudohyphae, and are 10-
40
41 40 micrometers in length and 5-10 micrometers in width.⁽⁸⁾ Candida parapsilosis in contrast present
42
43 as small hyper-reflective round 3-5 micrometers structures (Fig. 2C).⁽¹⁸⁾

44
45 Two recent studies^(14, 16) in patients with microbial keratitis demonstrated that IVCM had a
46
47 sensitivity from 89.2 to 94% and a specificity from 78 to 92.7% in patients with fungal keratitis. As
48
49 with Acanthamoeba keratitis, IVCM can be applied not only for diagnosis of fungal keratitis, but
50
51 for monitoring and guidance of treatment as well. In fungal keratitis, the depth of invasion is an
52
53 important prognostic factor, and IVCM is currently the only method that allows determination of
54
55 the depth of infection. This information helps the clinician to decide the timing for surgical
56
57 intervention when the disease is progressing despite medical treatment.⁽⁶⁾

58 Conclusion

59
60 IVCM is a non-invasive tool that may allow for rapid diagnoses of potentially blinding atypical
infections, such as Acanthamoeba and fungal keratitis, allowing prompt initiation of treatment.

1
2
3 IVCN may also provide the unique advantage of following the disease course and guiding
4 treatment, as well as shed light on the pathogenesis in these potentially devastating diseases.^(19, 20)
5
6 Currently smaller organisms, including bacteria and viruses are not visible on examination, and the
7 use of IVCN in these cases is not helpful. It is important to note that IVCN testing requires skilled
8 operators, and interpretation requires an experienced and well-trained observer. **Furthermore, in
9 some cases, the evidence of its high sensitivity and specificity is still poor and therefore IVCN
10 cannot at present replace microbiological testing.**⁽⁶⁾
11
12
13
14

15 *In Vivo Confocal Microscopy in Corneal Transplantation and Refractive Surgery*

16
17 IVCN is a valuable imaging modality for examining corneal cells and ultrastructure after
18 transplantation or other surgical procedures.
19

20
21 Confocal studies of the donor cornea after penetrating keratoplasty (PK) have revealed decreased
22 innervation,^(21, 23) increased backscatter,⁽²³⁾ and decreased cellularity.⁽²²⁾ With current interest in
23 lamellar keratoplasty techniques, this review will concentrate more on recent findings after lamellar
24 keratoplasty and other lamellar procedures.
25
26
27

28 Corneal Transplantation

29
30 Lamellar keratoplasty has resurged over the last decade for the treatment of anterior and
31 posterior corneal disease.⁽²⁴⁾ While donor changes would be similar to those after PK, corneas after
32 lamellar keratoplasty also contain residual host tissue and a new surgical lamellar interface.
33
34 Currently, the most common lamellar keratoplasty procedure is endothelial keratoplasty (EK),
35 specifically, Descemet stripping endothelial keratoplasty (DSEK), in which nearly all the host
36 cornea is retained with the exception of host Descemet membrane and endothelium. IVCN has
37 improved our knowledge of the residual changes in the host cornea after EK, and has enabled
38 understanding of some of the processes that affect the visual outcome after EK, as discussed below.
39
40
41
42
43

44 Corneal Backscatter after Corneal Transplantation

45
46 Corneal backscatter refers to light scattered toward an observer from the cornea and is of interest
47 after EK because backscatter from the surgical interface has been assumed to degrade postoperative
48 visual acuity.⁽²⁵⁾ With appropriate calibration of the incident light source and the optical detection
49 system, changes in corneal backscatter can be determined prospectively by using IVCN.⁽²⁶⁾ After
50 DSEK for Fuchs dystrophy, significant corneal backscatter is noted from the surgical interface in
51 the early period, but this decreases progressively over the first two years after surgery.⁽²⁷⁾ Contrary
52 to popular belief, backscatter from this region has not been associated with changes in visual acuity
53 or disability glare after EK.⁽²⁷⁾ In contrast, more backscatter can be measured from the subepithelial
54
55
56
57
58
59
60

1
2
3 and anterior stromal region of the cornea.^(27, 28) High backscatter in this region is present
4 preoperatively (in Fuchs dystrophy) and is caused by subtle basal epithelial edema, increased scatter
5 from the anterior stromal extracellular matrix, and the presence of subepithelial cells (presumed
6 fibroblasts), despite the cornea appearing clear by slit-lamp examination.⁽²⁹⁾ After DSEK, scatter
7 from this anterior region declines over the first six months, mainly because of resolution of
8 epithelial edema, but thereafter persists and remains elevated compared to normal through two years
9 after surgery. Scatter from the subepithelial region has not been associated with visual acuity after
10 DSEK, but has been associated with disability glare.^(25, 27, 30)

16 17 Corneal Cellularity after Corneal Transplantation

18
19 Corneal nerves are not affected by EK except those traversing the site of the incision,
20 whereas all the corneal nerves are severed during PK.^(22, 31) Nevertheless, IVCN has revealed
21 significant abnormalities of subbasal and stromal nerves before and after EK for Fuchs dystrophy.
22 Stromal nerves are frequently tortuous and closely associated with keratocytes, suggesting
23 interactions between these cell types.⁽³¹⁾ In addition, an abnormal and depleted subbasal nerve
24 plexus has been associated with decreased corneal sensitivity.^(31, 32)

25
26 Abnormal subepithelial cells (presumed fibroblasts) are brightly reflective cells visible before and
27 after DSEK for Fuchs dystrophy.⁽²⁹⁾ These cells contribute to corneal backscatter and possibly to
28 increased anterior surface aberrations.⁽³³⁾ Abnormalities of keratocytes, which repair and maintain
29 the cornealstroma, have been shown by IVCN. Keratocyte density is reduced in the most anterior
30 cornea in Fuchs dystrophy, and remains reduced with no evidence of repopulation through three
31 years after DSEK.^(29, 34) The consequence of this loss of cells is unknown, but possibly results in
32 impaired repair of the anterior stromal extracellular matrix after EK. Posterior host
33 keratocytensity has been found to decrease at two and three years after EK,⁽²⁹⁾ and might be the
34 consequence of loss of proximity, and therefore disrupted communication, between these cells and
35 the endothelial cells.

36
37 The donor corneal endothelium is easily examined by IVCN after EK, and it is an ideal imaging
38 technique for examining these thickened and potentially hazy corneas when compared to non-
39 contact specular microscopy.⁽³⁵⁾ Microfolds of the posterior donor cornea after EK can be visualized
40 by confocal microscopy, but these folds have not been associated with postoperative visual
41 acuity.⁽³⁶⁾

42 43 Excimer Keratorefractive Surgery

44
45 Laser in-situ keratomileusis (LASIK) and photorefractive keratectomy (PRK) are the most common
46 corneal surgical procedures. Both involve tissue removal by excimer photoablation, and LASIK
47
48
49
50
51
52
53
54
55
56
57
58
59
60

1
2
3 involves anterior corneal flap creation resulting in a lamellar interface.⁽³⁷⁾ Long-term changes in
4 corneal backscatter and cellularity in both procedures have been studied by IVCN.

7 Corneal Backscatter after Excimer Keratorefractive Surgery

8
9 Aside from transient increases in corneal backscatter in the early period after LASIK and
10 PRK, corneal backscatter is decreased over the longer-term, as measured by IVCN.^(26, 38) The
11 decrease can only be partly explained by decreased keratocyte density (see below). Other possible
12 factors are also thought to contribute to decreased reflectivity in the LASIK flap (unpublished data).
13 Of interest is that the anterior keratocyte depletion after LASIK and in Fuchs dystrophy is
14 associated with opposite effects on anterior corneal reflectivity.
15
16
17
18

19 Corneal Cellularity after Excimer Keratorefractive Surgery

20
21 Keratocyte density decreases after LASIK in the stromal flap, and after PRK, because of removal of
22 the highest density of anterior cells.⁽³⁹⁾ Loss of anterior keratocytes has not been associated with a
23 detrimental visual outcome, with increased backscatter, or with unstable anterior surface
24 aberrations.^(26, 40) Corneal subbasal nerves become depleted after LASIK and PRK, with a slow
25 recovery over several years, although decreased corneal sensitivity recovers within months.^(41, 42)
26 No long-term detrimental effects have been observed in the corneal endothelium by IVCN.^(43, 44)
27
28
29
30
31

32 ***In Vivo Confocal Microscopy of Ocular Surface in Dry Eye***

33
34 The International Dry Eye Workshop⁽⁴⁵⁾ (2007) and the International Workshop on Meibomian
35 Gland Dysfunction⁽⁴⁶⁾ (2010) recently defined dry eye and meibomian gland dysfunction (MGD).
36 Although these definitions provide clear descriptions of the disease components, in-depth
37 investigation of the pathophysiological mechanisms are still required.⁽⁴⁷⁾
38
39
40

41 IVCN is a minimally invasive and powerful tool which allows detection of changes in the ocular
42 surface epithelium, immune and inflammatory cells, corneal nerves, keratocytes, and meibomian
43 gland structures at cellular level.^(44, 45)
44
45

46 IVCN studies show dry eye-related changes in the corneal epithelium,⁽⁴⁹⁻⁵²⁾ including decreased
47 superficial cell density and increased basal density. Changes in the stroma are also evident by
48 IVCN including the presence of abnormal hyperreflective keratocytes.^(50, 53, 54) Some authors
49 referred to these as “activated” and interpreted them to be in a particular state of metabolic
50 activation, induced by proinflammatory mediators.^(50, 54, 55)
51
52
53
54

55 Confocal studies confirmed a key role of the sub-basal nerve plexus (SNP) in dry eye disease,
56 reporting increased tortuosity of the nerves.^(50, 51, 55) The nerves also show an increased density of
57 bead-like formations^(50, 51) that could reflect nerve damage or, alternatively, reflect increased
58
59
60

1
2
3 metabolic activity of nerve fibers in response to abnormal changes in the epithelium and to neuro-
4 inflammation. The meaning of changes in subbasal nerve tortuosity and bead-like formations is
5 currently subject to interpretation as there is conflicting data about those changes and how they
6 correlate with sensitivity.^(49, 50, 55-59) A more extensive discussion on this issue is included in the next
7 section.
8
9

10
11 IVCM demonstrated that the density of epithelial dendritic cells, which are interpreted as antigen
12 presenting cells, and other inflammatory cells increases in the central and peripheral cornea in
13 patients with dry eye.^(20, 60) Dynamic in vivo assessment of the central corneal inflammatory cell
14 density may not only be of help in evaluating dry eye severity, but can likely guide clinical
15 treatment and aid in the evaluation of the efficacy of anti-inflammatory drugs in clinical trials.^(47, 61)
16
17

18
19 IVCM has recently been used to examine the meibomian glands (MGs). With this application, it
20 provides a new tool to assess morphologic changes and allows the quantitative study of MG acinar
21 unit diameter and density, orifice diameter, and periglandular inflammatory cells density.⁽⁶²⁻⁶⁵⁾ The
22 method also allows semi-quantitative assessment of meibum secretion reflectivity and the
23 inhomogeneity of the glandular interstices and acinar wall.^(64, 65) Confocal data showed the potential
24 to diagnose simple MGD (Fig. 3) with high sensitivity and specificity and to assess MGD response
25 to treatment.⁽⁶³⁻⁶⁶⁾ Finally, confocal examination provided new information about particular patterns
26 of MG changes associated with Sjogren syndrome,⁽⁶⁴⁾ graft-versus-host disease,⁽⁶⁷⁾ contact lens
27 wear,⁽⁶⁵⁾ and aging.⁽⁶⁸⁾
28
29

30
31 Recent IVCM reports studied the conjunctiva in dry eye patients, focusing on confocal correlations
32 with impression cytology, inflammatory glands, and goblet cell evaluation. In Sjogren syndrome,
33 cellular changes resembling squamous metaplasia were present, and the mean cell area and nucleus-
34 cytoplasm ratio in impression cytology showed a significant correlation with the corresponding
35 confocal microscopy parameters (Figure 4).⁽⁶⁹⁾ IVCM was effective in the study of inflammatory
36 conjunctival cell density and response to treatment in Sjogren patients,^(70, 71) while data are
37 conflicting about the evaluation of goblet cells (repeatability, inter-observer agreement, images
38 interpretation and chances to discriminate these cells).^(70, 72) Finally, IVCM was successfully applied
39 to lacrimal gland examination in some Sjogren patients, revealing inflammatory cell infiltration and
40 perilobular fibrosis.⁽⁷³⁾
41
42
43
44
45
46
47
48
49
50
51

52
53 **In conclusion, IVCM is providing new opportunities to better understand the complex**
54 **pathophysiological mechanisms of dry eye. Recent confocal studies have shown several potential**
55 **clinical applications of this technology in the assessment of dry eye disease grading and prognosis,**
56
57
58
59
60

1
2
3 in the improvement of differential diagnosis, in the optimization of a tailored approach to treatment,
4 and in the evaluation of the responses to treatments.⁽⁷⁴⁾
5
6

7 *In Vivo Confocal Microscopy of Corneal Nerves*

8
9 The cornea is the most densely innervated tissue in the body with a density of nerve endings 200-
10 300 times greater than the skin.⁽⁷⁵⁾ The majority of nerves in the cornea have a sensory function.
11 Sensory nerve endings termed “nociceptors” function in maintaining homeostasis, in wound healing
12 and in sensing the environment to regulate tear secretion and distribution.
13
14

15
16 IVCM allows the description of the morphology, density, and disease- or surgically-induced
17 alterations of corneal nerves, particularly the subbasal nerve plexus.^(76, 77) It is particularly useful for
18 imaging corneal nerves near the corneal apex because the central cornea is more easily applanated
19 to obtain high quality tangential images. Although IVCM is capable of providing excellent images,
20 it lacks sufficient resolution to image nerve terminals in the epithelium and very small diameter
21 nerves in the subbasal plexus. Furthermore, the Heidelberg Engineering HRT laser scanning
22 confocal microscope that has been used in many of the published studies is only capable if imaging
23 a 400x400 µm area, making it difficult to locate and serially reimagine the same region of the cornea.
24
25
26
27
28
29

30 IVCM imaging of nerves in Ocular Surface and Corneal Diseases

31
32 IVCM has been used to image corneal nerves in a variety of corneal and ocular surface
33 diseases/conditions, including non-Sjögren syndrome (SS) or SS-associated aqueous tear
34 deficiency,^(49, 50, 56, 78) following LASIK surgery^(41, 79-84) (including post-LASIK dysesthesia) and
35 neurotrophic epitheliopathy before and after treatment with autologous serum.⁽⁸⁵⁾
36
37
38

39 Benitez del Castillo and associates reported decreased density of nerves in the subbasal
40 plexus in both non-SS and SS aqueous tear deficiency (ATD) compared to normal subjects < 60
41 years of age.⁽⁷⁸⁾ Furthermore, both ATD groups had a greater number of beaded nerves in the
42 subbasal plexus than control subjects less than and greater than age 60. Similar findings were also
43 observed by Villani and colleagues who reported a decreased number and increased tortuosity of
44 subbasal nerves compared to the control group.⁽⁵⁰⁾ Tuominen and colleagues observed nerve
45 sprouting in the SNP in 40% of eyes with SS.⁽⁴⁹⁾ The authors hypothesized that this finding may
46 represent sensory nerve regeneration. Nerve sprouting was noted in neonatal rat corneas after
47 treatment with capsaicin which induces release of neuropeptides from sensory nerve endings,⁽⁸⁶⁾ and
48 overexpression of nerve growth factor (NGF) was found to induce hypertrophy of the peripheral
49 nervous system.⁽⁸⁷⁾
50
51
52
53
54
55
56
57
58
59
60

1
2
3 In another study by Tuisku and associates, corneal subbasal nerve density was similar in patients
4 with SS and control subjects; however, thickening and cone-like structures were seen in nerves and
5 this was accompanied by hyperalgesia to an air jet esthesiometer and increased density of dendritic
6 cells (DC) surrounding corneal nerves in the SS corneas.⁽⁵⁶⁾ The density of DCs correlated with the
7 severity of irritation symptoms.
8
9

10 11 Post LASIK Hypoesthesia or Dysesthesia

12
13 Following LASIK, patients may rarely develop neurotrophic epitheliopathy or chronic pain, termed
14 “keratoneuralgia”.⁽⁸⁸⁻⁹⁰⁾ This may be due to abnormal regeneration or increased sodium ion channels
15 that lower the threshold to excitation, resulting in greater sensitivity to normal environmental
16 stimuli (e.g. air drafts, temperature change).⁽⁹⁰⁾ IVCN can confirm loss of corneal innervation or the
17 presence of abnormal nerve regeneration. It may identify patients who would benefit from
18 protective and/or regenerative therapy. Confocal microscopy of the cornea after LASIK has shown
19 decreased corneal nerve density in the early postoperative period that increases with time, albeit at a
20 slower rate than return of corneal sensitivity.⁽⁴¹⁾ The subbasal nerve fiber density is barely detectable
21 for up to six months post LASIK,⁽⁷⁹⁾ and one year after LASIK, the number of subbasal and stromal
22 nerves in the corneal flap are less than half the pre-operative density.⁽⁸⁰⁾ Immediately after LASIK,
23 most patients develop a relatively hypoesthetic cornea. Studies have found that corneal sensitivity
24 progressively improves and approaches the preoperative or “normal” range by 6-12 months when
25 measured with Cochet-Bonnet esthesiometry^(91, 92) and by up to 2 years when measured by gas
26 esthesiometry.⁽⁹³⁾
27
28

29
30 Nerve morphology has been found to correlate with corneal sensitivity after LASIK. One study
31 found that low sensitivity in specific corneal areas was associated not only with the absence of
32 nerves in confocal images, but also with short nerves lacking connections between nerve bundles.⁽⁸¹⁾
33 Another study found a significant association in LASIK patients between long nerve fiber bundles
34 and greater sensitivity by noncontact esthesiometry.⁽⁸²⁾ Finally, Stachs et al. concluded that
35 “normal” sensation returns to eyes by 6 months post-LASIK, despite a markedly abnormal SNP
36 with abnormally curved bundles or with thin nerves without the connections between nerve bundles
37 as seen in healthy, non-surgical eyes.⁽⁸³⁾
38
39

40
41 Tuisku et al. found that 2-5 years after LASIK for high myopia, most patients experienced ocular
42 surface discomfort consistent with dry eye syndrome, but in the absence of clinical signs of ocular
43 surface disease and with normal sensitivity measured with noncontact esthesiometry.⁽⁸⁴⁾ IVCN of
44 these corneas showed abnormal nerve morphology with excessive nerve sprouting. Interestingly,
45 patients with diabetes mellitus and severe peripheral neuropathy have also been found to have
46
47
48
49
50
51
52
53
54
55
56
57
58
59
60

1
2
3 tortuous subbasal nerves which may represent nerve regeneration.⁽⁸¹⁾ Many of the patients with post-
4 LASIK dysesthesia, evaluated at the Ocular Surface Center of the Cullen Eye Institute (Houston,
5 TX, USA), have an abnormal subbasal plexus with small, branched nerve bundles that lack
6 interconnections.
7
8

9 10 Neurotrophic Keratopathy

11
12 IVCN was found to be useful in monitoring corneas for evidence of nerve regeneration in patients
13 with neurotrophic keratopathy who were treated with autologous serum drops.⁽⁸⁵⁾ In a study
14 performed at the Ocular Surface Center of the Cullen Eye Institute (Houston, TX, USA), 11 eyes of
15 6 patients with neurotrophic keratopathy from a variety of conditions, including diabetes mellitus,
16 herpes zoster ophthalmicus and trigeminal nerve ablation were evaluated. Four images of the SNP
17 in the central cornea were randomly selected for analysis of the corneal nerves. Autologous plasma
18 drops were instilled 6 to 8 times per day. Autologous serum therapy resulted in improved best-
19 corrected visual acuity, decreased mean corneal fluorescein staining scores and significantly
20 increased corneal sensitivity measured by the Cochet-Bonnet and modified Belmonte
21 esthesiometers. The mean number, length, width and density of subbasal nerves increased
22 significantly after serum treatment.
23
24
25
26
27
28
29
30

31 These studies indicate that IVCN is a useful technology to image the SNP in normal and
32 diseased corneas. Additional studies are necessary to standardize examination methods and confirm
33 the findings of these preliminary studies.
34
35

36 Peripheral Neuropathy

37
38 A promising future clinical application of IVCN is the assessment and quantification of peripheral
39 neuropathies, related to diabetes mellitus or to other conditions known to cause small nerve fibre
40 damage, including hereditary sensory and autonomic neuropathy,⁽⁹⁴⁾ autoimmune neuropathy,⁽⁹⁵⁾
41 and chemotherapy-associated neuropathy.⁽⁹⁶⁾
42
43
44
45

46 Diabetic neuropathy, specifically, is a common and significant clinical problem, as highlighted by
47 The American Diabetes Association, which reports that 8.3% of US population is affected by
48 diabetes and that 60-70% of people with diabetes have mild to severe forms of nervous system
49 damage.⁽⁹⁷⁾ The accurate detection, characterization and quantification of this condition are
50 important in order to define at-risk patients, anticipate deterioration, monitor progression, assess
51 new therapies, and potentially reduce the incidence of foot ulcerations and amputations.⁽⁹⁸⁾
52
53
54
55

56 Several confocal studies reported corneal nerves changes in diabetic patients, including reduced
57 nerves density and branching and increased tortuosity.^(81, 99-101) The most recent researches showed
58
59
60

1
2
3 early detection,^(101, 102) severity stratification,^(100, 103) and moderate to high sensitivity and specificity
4 of IVCN for diagnosis of diabetic neuropathy^(99, 104), suggesting the prospect to use in vivo confocal
5 features of corneal nerves as biomarkers of diabetic neuropathy.^(105, 106) Larger longitudinal studies
6 and a larger normative database, together with ongoing IVCN technical progress, promise to allow
7 the optimization and diffusion of the clinical use of this approach.
8
9

10 *In Vivo Confocal Microscopy for Assessing the Ocular Surface in Glaucoma*

11
12 In glaucoma, IVCN constitutes an interesting aid to evaluate filtering blebs and to better
13 understand the conjunctival wound healing process. IVCN has also been used to assess corneal
14 changes induced by topical antiglaucoma medications and their preservatives.
15
16

17
18 The long-term success of glaucoma filtering surgery is mainly dependent on the development
19 of a functioning filtering bleb. The formation and the maintenance of this functioning bleb, with
20 regard to wound healing and conjunctival scarring, are therefore of primary importance. Because in
21 some cases the appearance of the bleb is not correlated to intraocular pressure (IOP) control and
22 because the reason of failure is often unclear, some authors have looked for new *in vivo* evaluation
23 techniques such as IVCN. This imaging technique allows the visualization of epithelial microcysts,
24 sub-epithelial connective tissue, blood vessels, and inflammatory cells within the conjunctival bleb
25 tissues.⁽¹⁰⁷⁻¹¹⁰⁾ Functioning blebs show a normal conjunctival epithelium with numerous microcysts
26 and a loose hyporeflexive sub-epithelial tissue with a high number of optically clear spaces. In
27 contrast, non-functioning blebs, show no or very few microcysts with hyper-reflective subepithelial
28 tissue, dense connective tissue and numerous blood vessels.^(107, 108) In functioning blebs with
29 mitomycin C, numerous clear spaces corresponding to large confluent microcysts and a loosely
30 arranged connective tissue with numerous large clear spaces may also be observed.^(107, 108, 110) The
31 infiltration of bleb tissues by inflammatory cells can be also observed and monitored during the
32 post-operative period.⁽¹⁰⁹⁾ Clinicians, with images at a cellular level, would be able to better predict
33 the outcome of these blebs and eventually provide specific treatments in order to enhance the
34 success rates of their surgical procedures.⁽¹⁰⁷⁾
35
36
37
38
39
40
41
42
43
44
45
46
47

48 Moreover, the chronic use of topical intraocular pressure (IOP)-lowering drugs and their
49 preservatives is known to cause significant changes in the ocular surface. Several studies have
50 evaluated the subbasal corneal nerves with IVCN in patients treated for glaucoma or ocular
51 hypertension. IVCN analysis showed ocular surface alterations in glaucomatous patients treated
52 chronically with Benzalkonium chloride (BAK)-containing eye drops. These changes included a
53 reduction of the density of superficial epithelial cells, activation of stromal keratocytes, decrease in
54 subbasal nerves and increase in subbasal nerve tortuosity.⁽¹¹¹⁾ Baratz *et al.* showed a decrease in the
55
56
57
58
59
60

1
2
3 number and density of subbasal corneal nerves in the medication group of the Ocular Hypertension
4 Treatment Study (OHTS).⁽¹¹²⁾ Martone *et al.* observed similar nerve modifications but in association
5 with an increased number of nerve beadings and tortuosity.⁽¹¹¹⁾ These authors also demonstrated a
6 direct relationship between nerve tortuosity and corneal sensation in glaucoma patients. Labbe *et al.*
7 recently evaluated the relationship between the *in vivo* confocal microscopic morphology of
8 subbasal corneal nerves and corneal sensitivity in patients with dry eye and patients treated for
9 glaucoma and ocular hypertension.⁽¹¹³⁾ The density and number of subbasal corneal nerves were
10 significantly decreased in dry eye and glaucoma patients compared to controls. In the dry eye
11 group, corneal sensitivity correlated with the density and the number of nerves. However, in the
12 glaucoma group, corneal sensitivity correlated only with the tortuosity of subbasal nerves. Although
13 patients with dry eyes and those medically treated for glaucoma experience similar ocular surface
14 symptoms and signs, the different correlations found between corneal sensation and nerve
15 morphology in these two groups suggest that nerve alterations and/or dysfunction could also be
16 different. Despite the decreased number of subbasal nerves observed in those patients, an additional
17 anesthetic effect of IOP-lowering medications and preservatives could explain these results.⁽¹¹³⁾

18
19
20 In relation to drug induced toxic effects, IVCN has also been widely used by researchers to
21 explore the ocular surface changes induced by topical medications and their preservatives. Clinical
22 observations of toxic keratopathy are important findings in glaucoma patients. Additionally IVCN
23 may be used in different animal models of ocular toxicity, in order to compare several formulations
24 of topical antiglaucoma eyedrops and preservatives.^(114, 115) Liang *et al.* also investigated with IVCN
25 the effects of antiglaucoma prostaglandin analogs with or without BAK preservative on the
26 conjunctiva-associated lymphoid tissue (CALT).⁽¹¹⁶⁾ The CALT reaction after instillation of BAK-
27 containing eye drops was characterized by inflammatory cell infiltration in the dome and
28 intrafollicular layers and by cell circulation inside the lymph vessels confirming the concentration-
29 dependent toxic effects of BAK. IVCN analyses of the ocular surface in animal models as well as
30 in humans could thus become pertinent tools in the future for evaluating and understanding
31 immunotoxicologic challenges on the ocular surface and would provide useful criteria for
32 investigating newly developed eye drops.

33 ***Confocal Microscopy in Contact Lens Wear***

34
35 IVCN has significantly enhanced our understanding of the ocular response to contact lens wear in
36 two ways. First, it has provided new perspectives, at a cellular level, on a wide range of contact
37 lens complications that have already been well documented in the literature, such as stromal edema
38 and changes in endothelial cell morphology. Second, it has revealed phenomena that were not
39
40
41
42
43
44
45
46
47
48
49
50
51
52
53
54
55
56
57
58
59
60

1
2
3 previously possible to image in the living human eye, such as the appearance of stromal microdots
4 and changes in keratocyte cell density. At present, IVCM is a precious complementary tool in
5 contact lens wearers' evaluation and management.⁽⁵³⁾ This technology, in addition to its previously
6 discussed essential role in contact lens related infectious keratitis, allows early detection of ocular
7 surface changes, finer identification of the pathogenic mechanisms, and improved tailored clinical
8 approach. As for several other areas, clinical utility of IVCM in contact lens wearers is suggested by
9 a strong background and supported by preliminary clinical experiences, but a satisfactory level of
10 evidence is still an unmet need. The following is a brief review of contact lens associated ocular
11 changes observed using IVCM in relation to the various substructures of the anterior eye.
12
13
14
15
16
17

18 Tear Film

19
20 Mucin balls form in the tear layer in patients wearing silicone hydrogel lenses. They have been
21 demonstrated using IVCM to vary in size from 40 μm to 80 μm ,⁽¹¹⁷⁾ and to display a highly
22 reflective core with a more poorly reflective, apparently translucent, outer layer.⁽¹¹⁸⁾ These
23 inclusions are spherical and can apparently penetrate the full thickness of the epithelium,^(117,119)
24 leading to activation of keratocytes in the underlying anterior stroma.⁽¹¹⁷⁾ Such observations indicate
25 a potential for mucin balls to render the cornea to be more susceptible to infection.
26
27
28
29
30

31 Corneal Epithelium

32
33 Epithelial cell size has been observed with the IVCM to increase in response to all forms of lens
34 wear, with the greatest effect seen in rigid lens wearers. Lenses of higher oxygen transmissibility
35 (Dk/t) have been shown to interfere least with the normal process of epithelial desquamation.⁽¹²⁰⁾
36 The degree of epithelial disturbance in response to various concentrations of preservatives used in
37 contact lens disinfecting solutions depends on the duration of lens wear.⁽¹²¹⁾ IVCM studies have
38 confirmed that extended wear of high Dk/t rigid lenses induces more epithelial thinning than
39 hydrogel lenses, which in turn induces more thinning than silicone hydrogel lenses.⁽¹²²⁾ Basal cell
40 morphology is unaffected by short⁽¹²³⁾ or long⁽¹²⁴⁾ term wear of high Dk/t soft lenses, but visible
41 alterations to basal cells (less regular in appearance) is associated with long term wear of low Dk/t
42 soft lenses.⁽¹²⁴⁾
43
44
45
46
47
48
49

50 Corneal Nerves

51
52 The current consensus is that contact lens wear does not alter corneal nerves;^(125,126) however, a
53 qualitative difference in appearance, such as slight blurring of nerves and less contrast with the
54 background, have been noted among contact lens wearers, which have been attributed to an artifact
55 due to lens-induced edema.⁽¹²⁷⁾
56
57
58
59
60

Corneal Dendritic Cells

Among contact lens wearers, a higher density of dendritic cells, which are presumed to be Langerhans' cells, occurs in the layer of the SNP in both the central and peripheral cornea. This suggests that contact lens wear can alter the immune status of the cornea.⁽¹²⁸⁾ Increased numbers of dendritic cells have also been observed in association with various combinations of soft contact lenses and lens care solutions.⁽¹²⁹⁾

Corneal Stroma

Dark lines and folds are observed with the IVCN in the edematous cornea in response to contact lens wear.⁽¹³⁰⁾ The lack of keratocyte clarity at high levels of edema probably corresponds with the corneal haze observed with the slit-lamp biomicroscope.⁽¹³⁰⁾ Apparent keratocyte loss following overnight lens wear⁽¹³¹⁾ is most likely an artifact due to uni-dimensional volumetric stromal expansion, causing keratocytes to be more 'spread out within the tissue. Consequently, when viewed by IVCN, fewer keratocytes are observed within the fixed depth of focus (this phenomenon can be explained by explained by the binomial expansion theory⁽¹³⁰⁾). As well, a degradation of image quality at higher levels of edema renders keratocytes more difficult to detect.⁽¹³⁰⁾ These artifacts need to be taken into account, or properly controlled for, in studies of keratocyte loss during contact lens wear.

Only a few of the studies that have investigated keratocyte loss associated with contact lens wear have attempted to account for these artifacts. Nevertheless, most of these studies have concluded that contact lens wear results in keratocyte apoptosis, although there is some disagreement as to the magnitude of this effect..^(125, 130-137) Mechanical stimulation of the corneal surface, due to the physical presence of a contact lens, and the consequent release of inflammatory mediators, is likely to be the main cause of the observed reduction in the number of keratocytes.^(133, 138) Keratocyte loss may play a role in contact lens-induced stromal thinning in view of the role of keratocytes in maintaining the structural integrity of the cornea.

Highly reflective stromal 'microdot deposits' can be observed with the IVCN throughout the entire stroma of lens wearers and non-lens wearers (Figure 7);⁽¹³⁹⁻¹⁴²⁾ however, **microdots appear in greater numbers in lens wearers and in patients with some disorders such as chloroquine induced keratopathy,⁽¹⁴³⁾ exfoliation syndrome⁽¹⁴⁴⁾ and mucopolysaccharidoses.⁽¹⁴⁵⁾ These findings' interpretation is still unclear in many cases and we may hypothesize that, in different conditions, similar images are due to different mechanisms. Contact lens related microdot deposits may represent granules of lipofuscin-like material within the corneal stroma of long-term contact lens wearers, formed as a result of chronic oxygen deprivation and chronic microtrauma to the cornea.**

Corneal Endothelium

Endothelial blebs are an acute response to lens wear which take on a different appearance with the IVCN compared with the slit lamp biomicroscope due to the different optical configuration of these two instruments. With the IVCN, endothelial blebs have a bright center and dark annular surround, set against a bright background field of the remainder of the 'non-blebbing' endothelium.⁽¹⁴²⁾

Optical models have been constructed to explain these differences.⁽¹⁴⁶⁾ Chronic morphological changes to the endothelium in response to lens wear observed with the IVCN,⁽¹⁴⁷⁾ such as increased polymegethism and increased light scatter, confirm previous observations made using specular microscopy.

Limbus

Long-term soft contact lens wear can induce many changes in corneal limbus, such as microcystic formations in epithelial cells, microdot deposits in corneal stroma, increased Langerhans cell density and decreased of keratocyte density.⁽¹⁴⁸⁾ There are more rolling leukocytes in limbal vessels in patients wearing low Dk/t lenses (versus non-lens-wearers),⁽¹⁴⁹⁾ highlighting the potential of this measure as an indication of sub-clinical inflammation.

Contact Lens Associated Keratitis

Because bacteria involved in contact lens related infections are beyond the resolution of the IVCN, this instrument cannot be used to diagnose contact lens-associated bacterial keratitis. However, the IVCN may be used to view damage to the various corneal layers caused by bacterial infection, such as needle-like deposits in crystalline keratitis,⁽¹⁵⁰⁾ and to indirectly assess the infectious process by monitoring the activity of Langerhans' cells.⁽¹⁵¹⁾

Contact lens wear is a significant risk factor for *Acanthamoeba* and fungal keratitis. IVCN role in these severe affections is discussed in a previous section of this review.

Investigation of the chronic morbidity of corneal infiltrative events associated with contact lens wear by IVCN revealed no significant impact upon basal epithelial cell density, anterior or posterior keratocyte density, or endothelial cell density, polymegethism or pleomorphism.⁽¹⁵²⁾

However, markedly reduced pan-corneal cell counts and increased endothelial polymegethism were observed in the affected eye of a patient who had suffered from a severe corneal infiltrative event.⁽¹⁵²⁾

Conjunctiva

Contact lens wear can induce changes in the bulbar conjunctiva as observed by IVCN. For instance, epithelial thinning, accelerated formation and enlargement of microcysts (Fig. 8), and increased

1
2
3 epithelial cell density occur and can be documented by IVCM.⁽¹⁵³⁾ A preliminary study found no
4 impact of soft contact lens wear on bulbar conjunctival goblet or Langerhans cell density.
5
6 Examination of MGs of contact lens wearers showed decreased basal epithelial cell density, lower
7
8 acinar unit diameters, higher glandular orifice diameters, greater secretion reflectivity and greater
9
10 inhomogeneity of the periglandular interstices.⁽⁶⁵⁾ These morphologic changes are interpreted as
11 signs of MGs dropout, duct obstruction, and glandular inflammation.⁽¹⁵⁴⁾
12

13 ***Advances in In Vivo Confocal Microscopy Imaging***

14
15 Current developments of IVCM include (1) 2 dimensional (D) wide field mapping, (2) 3D
16 reconstruction of the cornea, and (3) automated image analysis with the resulting quantification of
17 cornea parameters, including the SNP.
18
19

20 2D Wide Field Mapping

21
22 One of the crucial limitations of the confocal microscopy is the small field of imaging. Images
23 generated by confocal microscopes are relatively small (HRTII/RCM 400x400 μm ; Confoscan
24 4/Nidek 460x345 μm)⁽¹⁵⁵⁾ and contain only a very small portion of the SNP. The analysis of the
25 depicted nerve fibers may result in misleading findings after quantification. Therefore, several
26
27 studygroups are working on solutions with off- and on-line mapping procedures for corneal
28 structures.
29
30

31
32 Real-time mapping of the corneal emphasizing structures of the SNP was presented by Zhivov et
33 al.⁽¹⁵⁶⁾ Source data (384x384 pixels, 400x400 μm) were used to create large-scale maps of the
34 scanned area by selecting the Automatic Real Time (ART) composite mode. The algorithm is based
35 on an affine transformation. The maximal ART composite image size using source images is
36 3072x3072 pixels (3.2x3.2 mm) and corresponds to 8x8 non-overlapping images. The acquisition
37 time for a single composite image was up to 3 min. Given that the total CLSM time for a single
38 composite image is less than 3 min with no post-processing, the advantages of the online system are
39 apparent.
40
41

42
43 Another wide-field mapping technique was shown by Edwards et al.⁽¹⁵⁷⁾ The method uses the same
44 source data (384x384 pixels, 400x400 μm , max. number of 100 images, duration 20 sec) and
45 images could be mapped with a post-processing time of about 10 min.
46
47

48 3D Reconstruction

49
50 The idea for 3D imaging of the living cornea was originally suggested by Petroll *et al.* in 1993
51 when the first micrographs of rabbit cornea were published.⁽¹⁵⁸⁾ A further image processing
52 algorithm based on phase correlation was used by Allgeier et al.⁽¹⁵⁹⁾ to analyze and reduce motion
53
54
55
56
57
58
59
60

1
2
3 distortions in volume scan image sequences (30 images, volume depth 60 μm , constant interslice
4 distance 2 μm , duration 4 sec). 3D tracing of the SNP was performed in order to reconstruct images
5 containing only the SNP layer in humans.
6
7

8 Petrollet al. used the real time “streaming mode” of the HRT/RCM⁽¹⁶⁰⁾. A device modification
9 allowed z-scans through the whole thickness of the rabbit cornea with a 2 μm interslice distance.
10 The external software (ImageJ, <http://rsbweb.nih.gov/ij/>; Imaris, Bitplane Inc.) allowed the
11 determination of the epithelial and total corneal thickness as well as keratocyte density data.
12
13

14 Imaging and Quantification of the SNP

15 Presently, an automatic analysis of the SNP structures is the promising standard in SNP image
16 analysis. Zhivov et al.⁽¹⁶¹⁾ performed the evaluation of SNP on the basis of the best artifact-free
17 single image using in-house developed software tool. The analysis was based on morphological
18 (length, diameter, density) and topological (continuity and connectivity) parameters derived from
19 segmented nerve fibers. It also used the skeletonized medial lines that were transformed into
20 networks of undirected graphs consisting of nerve paths and various types of connecting nodes. A
21 more recent approach (Winter, unpublished) employs different local adaptive image filters for
22 image contrast homogenization during image pre-processing and an adapted Gabor filter model for
23 final image segmentation.
24
25

26 Dabbah et al.^(162, 163) presented an analysis and classification system for detecting nerve fibers in
27 confocal images. It was based on a multi-scale adaptive dual-model detection algorithm that
28 exploited the curvilinear structure of the nerve fibers and adapted itself to the local image
29 information. Holmes et al.⁽¹⁶⁴⁾ proposed a segmentation and skeletonization algorithm for the
30 detection of nerve fibers based on ridge map calculation. During the process nerve fibers are
31 identified, gaps are reconnected and finally quantified.
32

33 In summary, automated analysis of corneal nerve fibers employed and generated many
34 sophisticated methods and strategies in the field of medical image processing. Currently, a number
35 of different approaches in relation to the principal problem of small field of imaging of the SNP is
36 in progress which hopefully will provide promising solutions. Imaging of large areas of the SNP
37 will soon enable a considerably more accurate and thus more reliable quantification of nerve fiber
38 networks in the context of research and clinical diagnosis (Figure 9).
39
40
41
42
43

44 **Closing Remarks**

45 **The application of IVCM to the ocular surface opened a new era in ocular science.**
46
47
48
49
50
51
52
53
54
55
56
57
58
59
60

1
2
3 The slit lamp biomicroscopy has been the mainstay of ophthalmic examination of the anterior eye
4 for more than half a century, and this is unlikely to change. With its full colour, wide-field view,
5 low-to-medium magnification, binocular objective, highly versatile illumination system and
6 relatively low cost, the slit lamp will probably remain the instrument of first choice for examining
7 any ocular disease.⁽⁵³⁾
8
9

10
11 At present, IVCM provides new opportunities to view ocular surface structures at a cellular level,
12 through a quick, minimally-invasive (maybe non-invasive at all, in the next future), and steady-state
13 respectful examination.
14
15

16
17 The impact of IVCM on cornea and ocular surface research has been immediate and rapidly
18 growing, with 907 papers published from 1985 (when Lemp MA first reported confocal
19 examination of the cornea⁽¹⁶⁵⁾) to July 2013, 455 of them published in the last 5 years (data by
20 PubMed; research performed with the key-words “in vivo confocal microscopy cornea [OR] in vivo
21 confocal microscopy ocular surface”). This quantitative progression has been associated to a
22 qualitative evolution, moving from corneal apex to the whole ocular surface, from qualitative
23 assessments to attempts to standardize and, in some cases, automatize quantitative evaluations, from
24 small case series or pilot studies to well-constructed clinical trials.
25
26
27
28
29

30
31 Several challenges still remain. One of the main limitations of IVCM is the small field of view. In
32 vivo confocal microscopes currently used in ophthalmology can image only a very small area. For
33 instance, the HRTII/RCM (Heidelberg Engineering GmbH, Heidelberg, Germany) images a
34 400×400 μm field (0.160 mm²) and the Confoscan 4 ([NIDEK, Gamagori, Japan] images a
35 460×345 μm field (0.159 mm²). As a consequence of small fields of view and limitations of
36 applicability in eyes with small palpebral apertures, the reproducible investigation and
37 quantification of the same areas over time is virtually impossible. Additional concerns exist about
38 the standardization of image acquisition, interpretation, and quantification.⁽¹⁾
39
40
41
42
43

44
45 At present, these difficulties, together with the high cost of this technology, are factors preventing
46 widespread deployment and use of IVCM in clinical practice. However, despite the open
47 challenges, IVCM is ready to be used as a precious complementary in vivo technique for clinical
48 diagnosis and management and its clinical applications seem to be extremely promising and still
49 largely to be explored.
50
51
52
53
54
55
56
57
58
59
60

References

1. Niederer RL, McGhee CN. Clinical in vivo confocal microscopy of the human cornea in health and disease. *Progress in retinal and eye research*. 2010;29:30-58.
2. Guthoff RF, Zhivov A, Stachs O. In vivo confocal microscopy, an inner vision of the cornea - a major review. *Clin Experiment Ophthalmol*. 2009;37:100-17.
3. McLaren JW, Nau CB, Patel SV, Bourne WM. Measuring corneal thickness with the ConfoScan 4 and Z-ring adapter. *Eye Contact Lens*. 2007;33:185-190.
4. Thomas PA, Geraldine P. Infectious keratitis. *Curr Opin Infect Dis*. 2007; 20:129-141.
5. Keay L, Edwards K, Naduvilath T, Taylor HR, Snibson GR, Forde K, et al. Microbial keratitis predisposing factors and morbidity. *Ophthalmology*. 2006;113:109–116.
6. Kumar RL, Cruzat A, Hamrah P. Current state of in vivo confocal microscopy in management of microbial keratitis. *Semin Ophthalmol*. 2010;25:166-170.
7. Matsumoto Y, Dogru M, Sato EA, Katono Y, Uchino Y, Shimmura S, et al. The application of in vivo confocal scanning laser microscopy in the management of Acanthamoeba keratitis. *Mol Vis*. 2007;13:1319-26.
8. Labbé A, Khammari C, Dupas B, Gabison E, Brasnu E, Labetoulle M, et al. Contribution of in vivo confocal microscopy to the diagnosis and management of infectious keratitis. *Ocul Surf*. 2009;7:41-52.
9. Claerhout I, Goegebuer A, Van Den Broecke C, Kestelyn P. Delay in diagnosis and outcome of Acanthamoeba keratitis. *Graefes Arch Clin Exp Ophthalmol*. 2004;242:648-653.
10. Mathers WD, Nelson SE, Lane JL, Wilson ME, Allen RC, Folberg R. Confirmation of confocal microscopy diagnosis of Acanthamoeba keratitis using polymerase chain reaction analysis. *Arch Ophthalmol*. 2000;118:178-183.
11. Lee HJ, Alipour F, Cruzat A, Zheng L, Hamrah P. In vivo confocal microscopy in diagnosis and management of Acanthamoeba keratitis improves patient outcome. *Invest Ophthalmol Vis Sci*. 2010; 51: ARVO E-Abstract 2891.
12. Chew SJ, Feuerman RW, Assouline M, Kaufman HE, Barron BA, Hill JM. Early diagnosis of infectious keratitis with in vivo real time confocal microscopy. *CLAO J* 1992;18:197-201.
13. Kaufman SC, Musch DC, Belin MW, Cohen EJ, Meisler DM, Reinhart WJ, et al. Confocal microscopy: a report by the American Academy of Ophthalmology. *Ophthalmology*. 2004;111:396-406.

14. Kanavi MR, Javadi M, Yazdani S, Mirdehghanm S. Sensitivity and specificity of confocal scan in the diagnosis of infectious keratitis. *Cornea* 2007;26:782-786.
15. Tu EY, Joslin CE, Sugar J, Booton GC, Shoff ME, Fuerst PA. The relative value of confocal microscopy and superficial corneal scrapings in the diagnosis of *Acanthamoeba* keratitis. *Cornea*. 2008;27:764-772.
16. Vaddavalli PK, Garg P, Sharma S, Sangwan VS, Rao GN, Thomas R. Role of confocal microscopy in the diagnosis of fungal and *acanthamoeba* keratitis. *Ophthalmology*. 2011;118:29-35.
17. Hau SC, Dart JK, Vesaluoma M, Parmar DN, Claerhout I, Bibi K, et al. Diagnostic accuracy of microbial keratitis with in vivo scanning laser confocal microscopy. *Br J Ophthalmol*. 2010;94:982-987.
18. Baniyadi N, Cruzat A, Witkin D, Stacey R, Jakobiec FA, Chodosh J, et al. In vivo confocal microscopy for *Paecilomyces lilacinus* and *Candida parapsilosis* fungal keratitis. *Invest Ophthalmol Vis Sci*. 2011; 52: ARVO E-Abstract 5856.
19. Kurbanyan K, Hoesl LM, Schrems WA, Hamrah P. Corneal nerve alterations in acute *Acanthamoeba* and fungal keratitis: an in vivo confocal microscopy study. *Eye*. 2012; 26:126-132.
20. Cruzat A, Witkin D, Baniyadi N, Zheng L, Ciolino JB, Jurkunas UV, et al. Inflammation and the nervous system: the connection in the cornea in patients with infectious keratitis. *Invest Ophthalmol Vis Sci*. 2011; 52:5136-5143.
21. Hollingsworth JG, Efron N, Tullo AB. A longitudinal case series investigating cellular changes to the transplanted cornea using confocal microscopy. *Cont Lens Anterior Eye*. 2006;29:135-141.
22. Patel SV, Erie JC, McLaren JW, Bourne WM. Keratocyte density and recovery of subbasal nerves after penetrating keratoplasty and in late endothelial failure. *Arch Ophthalmol*. 2007;125:1693-1698.
23. Patel SV, McLaren JW, Hodge DO, Bourne WM. The effect of corneal light scatter on vision after penetrating keratoplasty. *Am J Ophthalmol*. 2008;146:913-919.
24. Tan DTH, Mehta JS. Future directions in lamellar corneal transplantation. *Cornea*. 2007;26(Suppl 1):S21-S28.
25. McLaren JW, Patel SV. Modeling the effect of forward scatter and aberrations on visual acuity after endothelial keratoplasty. *Invest Ophthalmol Vis Sci*. 2012;53:5545-5551.
26. McLaren JW, Bourne WM, Patel SV. Standardization of corneal haze measurement in confocal microscopy. *Invest Ophthalmol Vis Sci*. 2010;51:5610-5616.

- 1
- 2
- 3 27. Baratz KH, McLaren JW, Maguire LJ, Patel SV. Corneal haze determined by confocal
- 4 microscopy 2 years after Descemet stripping with endothelial keratoplasty for Fuchs corneal
- 5 dystrophy. *Arch Ophthalmol.* 2012;130:868-874.
- 6
- 7
- 8 28. Patel SV, Baratz KH, Hodge DO, Maguire LJ, McLaren JW. The effect of corneal light
- 9 scatter on vision after Descemet stripping with endothelial keratoplasty. *Arch Ophthalmol.*
- 10 2009;127:153-160.
- 11
- 12
- 13 29. Patel SV, McLaren JW. In vivo confocal microscopy of Fuchs endothelial dystrophy before
- 14 and after endothelial keratoplasty. *Arch Ophthalmol.* 2012; In Press.
- 15
- 16
- 17 30. van der Meulen IJ, Patel SV, Lapid-Gortzak R, Nieuwendaal CP, McLaren JW, van den
- 18 Berg TJ. Quality of vision in patients with Fuchs endothelial dystrophy and after Descemet
- 19 stripping endothelial keratoplasty. *Arch Ophthalmol.* 2011;129:1537-1542.
- 20
- 21
- 22 31. Ahuja Y, Baratz KH, McLaren JW, Bourne WM, Patel SV. Decreased corneal sensitivity
- 23 and abnormal corneal nerves in Fuchs endothelial dystrophy. *Cornea.* 2012;31:1257-1263.
- 24
- 25 32. Al-Aqaba M, Alomar T, Lowe J, Dua HS. Corneal nerve aberrations in bullous keratopathy.
- 26 *Am J Ophthalmol.* 2011;151:840-849.
- 27
- 28 33. Patel SV, Baratz KH, Maguire LJ, Hodge DO, McLaren JW. Anterior corneal aberrations
- 29 after Descemet stripping endothelial keratoplasty for Fuchs endothelial dystrophy.
- 30 *Ophthalmology,* 2012;119:1522-1529.
- 31
- 32
- 33 34. Hecker LA, McLaren JW, Bachman LA, Patel SV. Anterior keratocyte depletion in Fuchs
- 34 endothelial dystrophy. *Arch Ophthalmol.* 2011;129:555-561.
- 35
- 36 35. Raecker ME, McLaren JW, Kittleson KM, Patel SV. Endothelial image quality after
- 37 descemet stripping with endothelial keratoplasty: a comparison of three microscopy
- 38 techniques. *Eye Contact Lens.* 2011;37:6-10.
- 39
- 40
- 41 36. Seery LS, Nau CB, McLaren JW, Baratz KH, Patel SV. Graft thickness, graft folds, and
- 42 aberrations after descemet stripping endothelial keratoplasty for fuchs dystrophy. *Am J*
- 43 *Ophthalmol.* 2011;152:910-916.
- 44
- 45
- 46 37. Shortt AJ, Allan BD, Evans JR. Laser-assisted in-situ keratomileusis (LASIK) versus
- 47 photorefractive keratectomy (PRK) for myopia. *Cochrane Database Syst Rev.*
- 48 2013;1:CD005135.
- 49
- 50
- 51 38. McLaren JW, Bourne WM, Patel SV. Stromal reflectance after photorefractive keratectomy:
- 52 a paired comparison between epithelial removal by rotary brush and excimer laser-scrape.
- 53 *Invest Ophthalmol Vis Sci.* 2012;53(6):E-Abstract #1469.
- 54
- 55
- 56
- 57
- 58
- 59
- 60

- 1
2
3 39. Erie JC, Patel SV, McLaren JW, Hodge DO, Bourne WM. Corneal keratocyte deficits after
4 photorefractive keratectomy and laser in situ keratomileusis. *Am J Ophthalmol.*
5 2006;141:799-809.
6
7
- 8 40. Calvo R, McLaren JW, Hodge DO, Bourne WM, Patel SV. Corneal aberrations and visual
9 acuity after laser in situ keratomileusis: femtosecond laser versus mechanical
10 microkeratome. *Am J Ophthalmol.* 2010;149:785-793.
11
- 12 41. Erie JC, McLaren JW, Hodge DO, Bourne WM. Recovery of corneal subbasal nerve density
13 after PRK and LASIK. *Am J Ophthalmol.* 2005;140:1059-1064.
14
- 15 42. Patel SV, McLaren JW, Kittleson KM, Bourne WM. Subbasal nerve density and corneal
16 sensitivity after laser in situ keratomileusis: femtosecond laser versus mechanical
17 microkeratome. *Arch Ophthalmol.* 2010;128:1413-1419.
18
- 19 43. Klingler KN, McLaren JW, Bourne WM, Patel SV. Corneal endothelial cell changes 5 years
20 after laser in situ keratomileusis: femtosecond laser versus mechanical microkeratome. *J*
21 *Cataract Refract Surg.* 2012;38:2125-2130.
22
- 23 44. Patel SV, Bourne WM. Corneal endothelial cell loss 9 years after excimer laser
24 keratorefractive surgery. *Arch Ophthalmol.* 2009;127:1423-1427.
25
- 26 45. International Dry Eye WorkShop. The definition and classification of dry eye disease: report
27 of the Definition and Classification Subcommittee of the International Dry Eye Workshop
28 (2007). *Ocul Surf.* 2007;5:75–92.
29
- 30 46. Nichols KK, Foulks GN, Bron AJ, Glasgow BJ, Dogru M, Tsubota K, et al. The
31 international workshop on meibomian gland dysfunction: executive summary. *Invest*
32 *Ophthalmol Vis Sci.* 2011;52:1922–1929.
33
- 34 47. Alhatem A, Cavalcanti B, Hamrah P. In vivo confocal microscopy in dry eye disease and
35 related conditions. *SeminOphthalmol.* 2012;27:138-48.
36
- 37 48. Villani E, Magnani F, Viola F, Santaniello A, Scorza R, Nucci P, et al. In vivo confocal
38 evaluation of the ocular surface morpho-functional unit in dry eye. *Optom Vis Sci.*
39 2013;90:576-86.
40
- 41 49. Tuominen IS, Konttinen YT, Vesaluoma MH, Moilanen JA, Helintö M, Tervo TM. Corneal
42 innervation and morphology in primary Sjögren's syndrome. *Invest Ophthalmol Vis Sci.*
43 2003;44:2545–2549.
44
- 45 50. Villani E, Galimberti D, Viola F, Mapelli C, Ratiglia R. The cornea in Sjogren's syndrome:
46 an in vivo confocal study. *Invest Ophthalmol Vis Sci.* 2007;48:2017–2022.
47
48
49
50
51
52
53
54
55
56
57
58
59
60

- 1
2
3 51. Villani E, Galimberti D, Viola F, Mapelli C, Del Papa N, Ratiglia R. Corneal involvement in
4 rheumatoid arthritis: an in vivo confocal study. *Invest Ophthalmol Vis Sci.* 2008;49:560-
5 564.
6
- 7
8 52. Zhang X, Chen Q, Chen W, Cui L, Ma H, Lu F. Tear dynamics and corneal confocal
9
10
11
12
13 53. Efron N. Contact lens-induced changes in the anterior eye as observed in vivo with the
14
15
16
17 54. Villani E, Viola F, Sala R, Salvi M, Mapelli C, Currò N, et al. Corneal involvement in
18
19
20
21
22 55. Benítez del Castillo JM, Acosta MC, Wassfi MA, Díaz-Valle D, Gegúndez JA, Fernandez
23
24
25
26
27
28 56. Tuisku IS, Konttinen YT, Konttinen LM, Tervo TM. Alterations in corneal sensitivity and
29
30
31
32
33 57. Hoşal BM, Ornek N, Zilelioğlu G, Elhan AH. Morphology of corneal nerves and corneal
34
35
36
37 58. Zhang M, Chen J, Luo L, Xiao Q, Sun M, Liu Z. Altered corneal nerves in aqueous tear
38
39
40
41
42 59. Cruzat A, Pavan-Langston D, Hamrah P. In vivo confocal microscopy of corneal nerves—
43
44
45
46
47 60. Lin H, Li W, Dong N, Chen W, Liu J, Chen L, et al. Changes in corneal epithelial layer
48
49
50
51
52 61. Villani E, Galimberti D, Del Papa N, Nucci P, Ratiglia R. Inflammation in dry eye
53
54
55
56
57 62. Matsumoto Y, Sato EA, Ibrahim OM, Dogru M, Tsubota K. The application of in vivo laser
58
59
60

- 1
2
3 63. Ibrahim OM, Matsumoto Y, Dogru M, Adan ES, Wakamatsu TH, Goto T, et al. The
4 efficacy, sensitivity, and specificity of in vivo laser confocal microscopy in the diagnosis of
5 meibomian gland dysfunction. *Ophthalmology*. 2010;117:665-672.
6
7
8 64. Villani E, Beretta S, De Capitani M, Galimberti D, Viola F, Ratiglia R. In vivo confocal
9 microscopy of meibomian glands in Sjögren's syndrome. *Invest Ophthalmol Vis Sci*.
10 2011;52:933-939.
11
12 65. Villani E, Ceresara G, Beretta S, Magnani F, Viola F, Ratiglia R. In vivo confocal
13 microscopy of meibomian glands in contact lens wearers. *Invest Ophthalmol Vis Sci*.
14 2011;52:5215-5219.
15
16 66. Matsumoto Y, Shigeno Y, Sato EA, Ibrahim OM, Saiki M, Negishi K, et al. The evaluation
17 of the treatment response in obstructive meibomian gland disease by in vivo laser confocal
18 microscopy. *Graefes Arch Clin Exp Ophthalmol*. 2009;247:821-829.
19
20 67. Ban Y, Ogawa Y, Ibrahim OM, Tatematsu Y, Kamoi M, Uchino M, et al. Morphologic
21 evaluation of meibomian glands in chronic graft-versus-host disease using in vivo laser
22 confocal microscopy. *Mol Vis*. 2011;17:2533-2543.
23
24 68. Villani E, Canton V, Magnani F, Viola F, Nucci P, Ratiglia R. The aging meibomian gland:
25 an in vivo confocal study. *Invest Ophthalmol Vis Sci*. 2013;54:4735-40.
26
27 69. Kojima T, Matsumoto Y, Dogru M, Tsubota K. The application of in vivo laser scanning
28 confocal microscopy as a tool of conjunctival in vivo cytology in the diagnosis of dry eye
29 ocular surface disease. *Mol Vis*. 2010;16:2457-2464.
30
31 70. Villani E, Beretta S, Galimberti D, Viola F, Ratiglia R. In vivo confocal microscopy of
32 conjunctival roundish bright objects: young, older, and Sjögren subjects. *Invest Ophthalmol*
33 *Vis Sci*. 2011;52:4829-4832.
34
35 71. Wakamatsu TH, Sato EA, Matsumoto Y, Ibrahim OM, Dogru M, Kaido M, et al.
36 Conjunctival in vivo confocal scanning laser microscopy in patients with Sjögren syndrome.
37 *Invest Ophthalmol Vis Sci*. 2010;51:144-150.
38
39 72. Hong J, Zhu W, Zhuang H, Xu J, Sun X, Le Q, et al. In vivo confocal microscopy of
40 conjunctival goblet cells in patients with Sjögren's syndrome dry eye. *Br J Ophthalmol*.
41 2010;94:1454-1458.
42
43 73. Sato EA, Matsumoto Y, Dogru M, Kaido M, Wakamatsu T, Ibrahim OM, et al. Lacrimal
44 gland in Sjögren's syndrome. *Ophthalmology*. 2010;117:1055-1055.
45
46 74. Villani E, Mantelli F, Nucci P. In vivo confocal microscopy of the ocular surface: ocular
47 allergy and dry eye. *Curr Opin Allergy Clin Immunol*. In press.
48
49
50
51
52
53
54
55
56
57
58
59
60

- 1
- 2
- 3 75. Kenchegowda S, Bazan HE. Significance of lipid mediators in corneal injury and repair. *J*
- 4 *Lipid Res.* 2010;51:879-891.
- 5
- 6 76. Oliveira-Soto L, Efron N. Morphology of corneal nerves using confocal microscopy.
- 7 *Cornea.* 2001;20:374-384.
- 8
- 9
- 10 77. Patel DV, McGhee CN. In vivo confocal microscopy of human corneal nerves in health, in
- 11 ocular and systemic disease, and following corneal surgery: a review. *Br J Ophthalmol.*
- 12 2009;93:853-860.
- 13
- 14 78. Benítez del Castillo JM, Wasfy MA, Fernandez C, Garcia-Sanchez J. An in vivo confocal
- 15 masked study on corneal epithelium and subbasal nerves in patients with dry eye. *Invest*
- 16 *Ophthalmol Vis Sci.* 2004;45:3030-3035.
- 17
- 18 79. Lee SJ, Jin KK, Kyung YS, Kim EK, Lee HK. Comparison of corneal nerve regeneration
- 19 and sensitivity between LASIK and laser epithelial keratomileusis (LASEK). *Am J*
- 20 *Ophthalmol.* 2006;141:1009-1015.
- 21
- 22
- 23 80. Lee BH, McLaren JW, Erie JC, Hodge DO, Bourne WM. Reinnervation in the cornea after
- 24 LASIK. *Invest Ophthalmol Vis Sci.* 2002;43:3660-3664.
- 25
- 26 81. Kallinikos P, Berhanu M, O'Donnell C, Boulton AJ, Efron N, Malik RA. Corneal nerve
- 27 tortuosity in diabetic patients with neuropathy. *Invest Ophthalmol Vis Sci.* 2004;45:418-
- 28 422.
- 29
- 30 82. Stapleton F, Hayward KB, Bachand N, Trong PH, Teh DW, Deng KM, et al. Evaluation of
- 31 corneal sensitivity to mechanical and chemical stimuli after LASIK: a pilot study. *Eye*
- 32 *Contact Lens.* 2006;32:88-93.
- 33
- 34 83. Stachs O, Zhivov A, Kraak R, Hovakimyan M, Wree A, Guthoff R. Structural-functional
- 35 correlations of corneal innervation after LASIK and penetrating keratoplasty. *J Refrac Surg.*
- 36 2010;26:159-167.
- 37
- 38 84. Tuisku IS, Lindbohm N, Wilson SE. Dry eye and corneal sensitivity after high myopic
- 39 LASIK. *J Refract Surg.* 2007;23:338-342.
- 40
- 41 85. Rao K, Leveque C, Pflugfelder SC. Corneal nerve regeneration in neurotrophic keratopathy
- 42 following autologous plasma therapy. *Br J Ophthalmol.* 2010;94:584-591.
- 43
- 44 86. Marfurt CF, Ellis LC, Jones MA. Sensory and sympathetic nerve sprouting in the rat cornea
- 45 following neonatal administration of capsaicin. *Somatosens Mot Res.* 1993;10:377-398.
- 46
- 47 87. Albers KM, Wright DE, Davis BM. Overexpression of nerve growth factor in epidermis of
- 48 transgenic mice causes hypertrophy of the peripheral nervous system. *J Neurosci.*
- 49 1994;14:1422-1432.
- 50
- 51
- 52
- 53
- 54
- 55
- 56
- 57
- 58
- 59
- 60

- 1
2
3 88. Ambrósio R Jr, Tervo T, Wilson SE. LASIK-associated dry eye and neurotrophic
4 epitheliopathy: pathophysiology and strategies for prevention and treatment. *J Refract Surg.*
5 2008;24:396-407.
6
- 7
8 89. Rosenthal P, Baran I, Jacobs DS. Corneal pain without stain. Is it real? *Ocul Surf* 2009;7:28-
9 40.
10
- 11 90. Nettune GR, Pflugfelder SC. Post-LASIK tear dysfunction and dysesthesia. *Ocular Surf.*
12 2010; 8:135-145.
13
- 14 91. Benitez-del-Castillo JM, del Rio T, Iradier T, Hernández JL, Castillo A, Garcia-Sanchez J.
15 Decrease in tear secretion and corneal sensitivity after laser in situ keratomileusis. *Cornea.*
16 2001; 20:30-32.
17
- 18 92. Battat L, Macri A, Dursun D, Pflugfelder SC. Effects of laser in situ keratomileusis on tear
19 production, clearance, and the ocular surface. *Ophthalmology.* 2001;108:1230-1235.
20
- 21 93. Gallar J, Acosta MC, Moilanen JA, Holopainen JM, Belmonte C, Tervo TM. Recovery of
22 corneal sensitivity to mechanical and chemical stimulation after laser in situ keratomileusis.
23 *J Refract Surg.* 2004;20:229-235.
24
- 25 94. Mimura T, Amano S, Fukuoka S, Honda N, Arita R, Ochiai M, et al. In vivo confocal
26 microscopy of hereditary sensory and autonomic neuropathy. *Curr Eye Res* 2008;33:940-
27 945.
28
- 29 95. Lalive PH, Truffert A, Magistris MR, Landis T, Dosso A. Peripheral autoimmune
30 neuropathy assessed using corneal in vivo confocal microscopy. *Arch Neurol* 2009;66:403-
31 405.
32
- 33 96. Ferrari G, Gemignani F, Macaluso C. Chemotherapy-associated peripheral sensory
34 neuropathy assessed using in vivo corneal confocal microscopy. *Arch Neurol* 2010;67:364-
35 365.
36
- 37 97. American Diabetes Association. Data from the 2011 National Diabetes Fact Sheet.
38 Available at [http://www.diabetes.org/diabetes-basics/diabetes-](http://www.diabetes.org/diabetes-basics/diabetes-statistics/?loc=DropDownDB-stats)
39 [statistics/?loc=DropDownDB-stats.](http://www.diabetes.org/diabetes-basics/diabetes-statistics/?loc=DropDownDB-stats)
40
- 41 98. Abbott CA, Vileikyte L, Williamson S, Carrington AL, Boulton AJ. Multicenter study of the
42 incidence of and predictive risk factors for diabetic neuropathic foot ulceration. *Diabetes*
43 *Care* 1998;21:1071-5.
44
- 45 99. Tavakoli M, Quattrini C, Abbott CA, Kallinikos P, Marshall A, Finnigan J, et al. Corneal
46 confocal microscopy: a novel noninvasive test to diagnose and stratify the severity of human
47 diabetic neuropathy. *Diabetes Care* 2010;33:1792-1797.
48
49
50
51
52
53
54
55
56
57
58
59
60

- 1
2
3 100. Rosenberg ME, Tervo TM, Immonen IJ, Müller LJ, Grönhagen-Riska C, Vesaluoma
4 MH. Corneal structure and sensitivity in type 1 diabetes mellitus. *Invest Ophthalmol Vis Sci*
5 2000;41:2915-21.
6
7
8 101. Mocan MC, Durukan I, Irkec M, Orhan M. Morphologic alterations of both the
9 stromal and subbasal nerves in the corneas of patients with diabetes. *Cornea* 2006;25:769-
10 73.
11
12 102. Ziegler D, Zhivov A, Allgeier S, Winter K, Papanas N, Ziegler I, et al. Early
13 detection of nerve fiber loss by corneal confocal microscopy and skin biopsy in recently
14 diagnosed type 2 diabetic subjects. *Diabetologia*. 2012;55 Suppl 1:A44.
15
16 103. Petropoulos IN, Alam U, Fadavi H, Asghar O, Green P, Ponirakis G, et al. Corneal
17 Nerve Loss Detected With Corneal Confocal Microscopy Is Symmetrical and Related to the
18 Severity of Diabetic Polyneuropathy. *Diabetes Care*. 2013 Jul 22. [Epub ahead of print]
19
20 104. Ahmed A, Bril V, Orszag A, Paulson J, Yeung E, Ngo M, et al. Detection of diabetic
21 sensorimotor polyneuropathy by corneal confocal microscopy in type 1 diabetes: a
22 concurrent validity study. *Diabetes Care*. 2012;35:821–8.
23
24 105. Pritchard N, Edwards K, Shahidi AM, Sampson GP, Russell AW, Malik RA, et al.
25 Corneal markers of diabetic neuropathy. *Ocul Surf*. 2011;9:17-28.
26
27 106. Papanas N, Ziegler D. Corneal confocal microscopy: a new technique for early
28 detection of diabetic neuropathy. *Curr Diab Rep*. 2013;13:488-99.
29
30 107. Labbe A, Dupas B, Hamard P, Baudouin C. In vivo confocal microscopy study of
31 blebs after filtering surgery. *Ophthalmology*. 2005;112:1979.
32
33 108. Guthoff R, Klink T, Schlunck G, Grehn F. In vivo confocal microscopy of failing
34 and functioning filtering blebs: Results and clinical correlations. *J Glaucoma* 2006;15:552-
35 558.
36
37 109. Messmer EM, Zapp DM, Mackert MJ, Thiel M, Kampik A. In vivo confocal
38 microscopy of filtering blebs after trabeculectomy. *Arch Ophthalmol*. 2006;124:1095-1103.
39
40 110. Amar N, Labbe A, Hamard P, Dupas B, Baudouin C. Filtering blebs and aqueous
41 pathway an immunocytological and in vivo confocal microscopy study. *Ophthalmology*.
42 2008;115:1154-1161.e4.
43
44 111. Martone G, Frezzotti P, Tosi GM, Traversi C, Mittica V, Malandrini A, et al. An in
45 vivo confocal microscopy analysis of effects of topical antiglaucoma therapy with
46 preservative on corneal innervation and morphology. *Am J Ophthalmol*. 2009;147:725-735.
47
48
49
50
51
52
53
54
55
56
57
58
59
60

- 1
2
3
4
5
6
7
8
9
10
11
12
13
14
15
16
17
18
19
20
21
22
23
24
25
26
27
28
29
30
31
32
33
34
35
36
37
38
39
40
41
42
43
44
45
46
47
48
49
50
51
52
53
54
55
56
57
58
59
60
112. Baratz KH, Nau CB, Winter EJ, McLaren JW, Hodge DO, Herman DC, et al. Effects of glaucoma medications on corneal endothelium, keratocytes, and subbasal nerves among participants in the ocular hypertension treatment study. *Cornea*. 2006;25:1046-1052.
 113. Labbe A, Alalwani H, Van Went C, Brasnu E, Georgescu D, Baudouin C. The relationship between subbasal nerve morphology and corneal sensation in ocular surface disease. *Invest Ophthalmol Vis Sci*. 2012;53:4926-4931.
 114. Liang H, Brignole-Baudouin F, Riancho L, Baudouin C. Reduced in vivo ocular surface toxicity with polyquad-preserved travoprost versus benzalkonium-preserved travoprost or latanoprost ophthalmic solutions. *Ophthalmic Res*. 2012;48:89-101.
 115. Labbe A, Pauly A, Liang H, Brignole-Baudouin F, Martin C, Warnet JM, et al. Comparison of toxicological profiles of benzalkonium chloride and polyquaternium-1: an experimental study. *J Ocul Pharmacol Ther*. 2006;22:267-278.
 116. Liang H, Baudouin C, Labbe A, Riancho L, Brignole-Baudouin F. Conjunctiva-associated lymphoid tissue (CALT) reactions to antiglaucoma prostaglandins with or without BAK-preservative in rabbit acute toxicity study. *PLoS One* 2012;7:e33913.
 117. Ladage PM, Petroll WM, Jester JV, Fisher S, Bergmanson JP, Cavanagh HD. Spherical indentations of human and rabbit corneal epithelium following extended contact lens wear. *CLAO J*. 2002;28:177-180.
 118. Craig JP, Sherwin T, Grupcheva CN, McGhee CN. An evaluation of mucin balls associated with high-DK silicone-hydrogel contact lens wear. *Adv Exp Med Biol*. 2002;506:917-923.
 119. Millar TJ, Papas EB, Ozkan J, Jalbert I, Ball M. Clinical appearance and microscopic analysis of mucin balls associated with contact lens wear. *Cornea*. 2003;22:740-745.
 120. Ladage PM, Yamamoto K, Ren DH, Li L, Jester JV, Petroll WM. Effects of rigid and soft contact lens daily wear on corneal epithelium, tear lactate dehydrogenase, and bacterial binding to exfoliated epithelial cells. *Ophthalmology*. 2001;108:1279-1288.
 121. Imayasu M, Moriyama T, Ichijima H, Ohashi J, Petroll WM, Jester JV, et al. The effects of daily wear of rigid gas permeable contact lenses treated with contact lens care solutions containing preservatives on the rabbit cornea. *CLAO J*. 1994;20:183-188.
 122. Ren DH, Petroll WM, Jester JV, Ho-Fan J, Cavanagh HD. The relationship between contact lens oxygen permeability and binding of *Pseudomonas aeruginosa* to human corneal epithelial cells after overnight and extended wear. *CLAO J*. 1999;25:80-100. Erratum 25:175.

- 1
2
3 123. Kalogeropoulos G, Chang S, Bolton T, Jalbert I. The effects of short-term lens wear and
4 eye rubbing on the corneal epithelium. *Eye Contact Lens*. 2009;35:255-259.
5
6 124. Jalbert I, Sweeney DF, Stapleton F. The effect of long-term wear of soft lenses of low and
7 high oxygen transmissibility on the corneal epithelium. *Eye (Lond)*. 2009;23:1282-1287.
8
9 125. Bansal AK, Mustonen RK, McDonald MB. High resolution in vivo scanning confocal
10 microscopy of the cornea in long term contact lens wear. *Invest Ophthalmol Vis Sci*.
11 1997;38:S138.
12
13 126. Wu T, Ahmed A, Bril V, Orszag A, Ng E, Nwe P et al. Variables associated with corneal
14 confocal microscopy parameters in healthy volunteers: implications for diabetic neuropathy
15 screening. *Diabet Med*. 2012;29:e297-e303.
16
17 127. Oliveira-Soto L, Efron N. Morphology of corneal nerves in soft contact lens wear. A
18 comparative study using confocal microscopy. *Ophthal Physiol Opt*. 2003;23:163-174.
19
20 128. Zhivov A, Stave J, Vollmar B, Guthoff R. In vivo confocal microscopic evaluation of
21 langerhans cell density and distribution in the corneal epithelium of healthy volunteers and
22 contact lens wearers. *Cornea*. 2007;26:47-54.
23
24 129. Sindt CW, Grout TK, Critser DB, Kern JR, Meadows DL. Dendritic immune cell densities
25 in the central cornea associated with soft contact lens types and lens care solution types: a
26 pilot study. *Clin Ophthalmol*. 2012;6:511-519.
27
28 130. Efron N, Mutalib HA, Perez-Gomez I, Koh HH. Confocal microscopic observations of the
29 human cornea following overnight contact lens wear. *Clin Exp Optom*. 2002;85:149-155.
30
31 131. Patel SV, McLaren JW, Hodge DO, Bourne WM. Confocal microscopy in vivo in corneas
32 of long-term contact lens wearers. *Invest Ophthalmol Vis Sci*. 2002;43:995-1003.
33
34 132. Jalbert I, Stapleton F. Effect of lens wear on corneal stroma: preliminary findings. *Aust N*
35 *Z J Ophthalmol*. 1999;27:211-213.
36
37 133. Kallinikos P, Morgan PB, Efron N. Assessment of stromal keratocytes and tear film
38 inflammatory mediators during extended wear of contact lenses. *Cornea*. 2006;25:1-10.
39
40 134. Weed KH, MacEwen CJ, Cox A, McGhee CN. Quantitative analysis of corneal
41 microstructure in keratoconus utilising in vivo confocal microscopy. *Eye (Lond)*.
42 2007;21:614-623.
43
44 135. Zhong X, Chen X, Xie RZ, Yang J, Li S, Yang X, et al. Differences between overnight
45 and long-term wear of orthokeratology contact lenses in corneal contour, thickness, and cell
46 density. *Cornea*. 2009;28:271-279.
47
48 136. Yagmur M, Okay O, Sizmaz S, Unal I, Yar K. In vivo confocal microscopy: corneal
49 changes of hydrogel contact lens wearers. *Int Ophthalmol*. 2011;31:377-383.
50
51
52
53
54
55
56
57
58
59
60

- 1
2
3 137. Ohta K, Shimamura I, Shiraishi A, Ohashi Y. Confocal microscopic observations of
4 stromal keratocytes in soft and rigid contact lens wearers. *Cornea*. 2012;31:66-73.
5
6 138. Kallinikos P, Efron N. On the etiology of keratocyte loss during contact lens wear. *Invest*
7 *Ophthalmol Vis Sci*. 2004;45:3011-3020.
8
9 139. Böhnke M, Masters BR. Long term contact lens wear induces a corneal degeneration with
10 microdot deposits in the corneal stroma. *Ophthalmology*. 1997;104:1887-1896.
11
12 140. Trittibach P, Cadez R, Eschmann R, Sarra GM, Boehnke M, Frueh BE. Determination of
13 microdot stromal degenerations within corneas of long-term contact lens wearers by
14 confocal microscopy. *Eye Contact Lens*. 2004;30:127-131.
15
16 141. Bastion ML, Mohamad MH. Study of the factors associated with the presence of white
17 dots in the corneas of regular soft contact lens users from an Asian country. *Eye Contact*
18 *Lens*. 2006;32:223-227.
19
20 142. Efron N, Mutalib HA. Confocal microscopy observations of the cornea in response to
21 contact lens wear. *dieKontaktlinse* 2001;35:4-16.
22
23 143. Ma X, He L, He D, Xu J. Chloroquine keratopathy of rheumatoid arthritis patients
24 detected by in vivo confocal microscopy. *Curr Eye Res*. 2012;37:293-9.
25
26 144. Sbeity Z, Palmiero PM, Tello C, Liebmann JM, Ritch R. Non-contact in vivo confocal
27 scanning laser microscopy in exfoliation syndrome, exfoliation syndrome suspect and
28 normal eyes. *Acta Ophthalmol*. 2011;89:241-7.
29
30 145. Mocan MC, Eldem B, Irkec M. In vivo confocal microscopic findings of two siblings with
31 Maroteaux-Lamy syndrome. *Cornea*. 2007;26:90-3.
32
33 146. Efron N. Endothelial blebs. In: Efron N au. *Contact Lens Complications*. 3rd ed.
34 Edinburgh: Elsevier-Saunders; 2012.
35
36 147. Nagel S, Wiegand W, Thaer AA, Geyer OC. Light scattering study of the cornea in
37 contact lens patients. In vivo studies using confocal slit scanning microscopy.
38 *Ophthalmologe*. 1996;93:252-256.
39
40 148. Rong B, Yan XM. Changes of corneal limbus in long-term soft contact lens wearers by
41 using laser confocal microscope. *Zhonghua Yan KeZaZhi*. 2007;43:514-518.
42
43 149. Nguyen TH, Dudek LT, Krisciunas TC, Matiaco P, Planck SR, Mathers WD, et al. In vivo
44 confocal microscopy: increased conjunctival or episcleral leukocyte adhesion in patients
45 who wear contact lenses with lower oxygen permeability (Dk) values. *Cornea*. 2004;23:695-
46 700.
47
48 150. Sutphin JE, Kantor AL, Mathers WD, Mehaffey MG. Evaluation of infectious crystalline
49 keratitis with confocal microscopy in a case series. *Cornea*. 1997;16:21-26.
50
51
52
53
54
55
56
57
58
59
60

- 1
2
3 151. Su PY, Hu FR, Chen YM, Han JH, Chen WL. Dendritiform cells found in central cornea
4 by in-vivo confocal microscopy in a patient with mixed bacterial keratitis. *Ocul Immunol*
5 *Inflamm.* 2006;14:241-244.
6
7
8 152. Efron N, Morgan PB, Makrynioti D. Chronic morbidity of corneal infiltrative events
9 associated with contact lens wear. *Cornea.* 2007;26:793-799.
10
11 153. Efron N, Al-Dossari M, Pritchard N. Confocal microscopy of the bulbar conjunctiva in
12 contact lens wear. *Cornea.* 2010;29:43-52.
13
14 154. Arita R, Itoh K, Inoue K, Kuchiba A, Yamaguchi T, Amano S. Contact lens wear is
15 associated with decrease of meibomian glands. *Ophthalmology.* 2009;116:379-84.
16
17 155. Zhivov A, Stachs O, Stave J, Guthoff RF. In vivo three-dimensional confocal laser
18 scanning microscopy of corneal surface and epithelium. *Br J Ophthalmol.* 2009;93:667-672.
19
20 156. Zhivov A, Blum M, Guthoff R, Stachs O. Real-time mapping of the subepithelial nerve
21 plexus by in vivo confocal laser scanning microscopy. *Br J Ophthalmol.* 2010;94:1133-
22 1135.
23
24 157. Edwards K, Pritchard N, Gosschalk K, Sampson GP, Russell A, Malik RA, et al. Wide-
25 field assessment of the human corneal subbasal nerve plexus in diabetic neuropathy using a
26 novel mapping technique. *Cornea.* 2012;31:1078-1082.
27
28 158. Petroll WM, Cavanagh HD, Jester JV. Three-dimensional imaging of corneal cells using
29 in vivo confocal microscopy. *J Microsc.* 1993;170:213-219.
30
31 159. Allgeier S, Zhivov A, Eberle F, Koehler B, Maier S, Bretthauer G, et al. Image
32 reconstruction of the subbasal nerve plexus with in vivo confocal microscopy. *Invest*
33 *Ophthalmol Vis Sci.* 2011;52:5022-5028.
34
35 160. Petroll WM, Weaver M, Vaidya S, McCulley JP, Cavanagh HD. Quantitative 3-
36 Dimensional Corneal Imaging In Vivo Using a Modified HRT-RCM Confocal Microscope.
37 *Cornea.* 2013;32:e36-e43.
38
39 161. Zhivov A, Winter K, Peschel S, Guthoff RF, Stachs O, Harder V, et al. [Quantitative
40 analysis of corneal subbasal nerve plexus with in vivo confocal laser scanning microscopy].
41 *Klin Monbl Augenheilkd.* 2011;228:1067-1072.
42
43 162. Dabbah MA, Graham J, Petropoulos IN, Tavakoli M, Malik RA. Automatic analysis of
44 diabetic peripheral neuropathy using multi-scale quantitative morphology of nerve fibres in
45 corneal confocal microscopy imaging. *Med Image Anal.* 2011;15:738-47.
46
47 163. Dabbah MA, Graham J, Petropoulos I, Tavakoli M, Malik RA. Dual-model automatic
48 detection of nerve-fibres in corneal confocal microscopy images. *Med Image Comput*
49 *Comput Assist Interv.* 2010;13:300-7.
50
51
52
53
54
55
56
57
58
59
60

- 1
2
3 164. Holmes TJ, Pellegrini M, Miller C, Epplin-Zapf T, Larkin S, Luccarelli S, et al.
4 Automated software analysis of corneal micrographs for peripheral neuropathy. Invest
5 Ophthalmol Vis Sci. 2010;51:4480-91.
6
7
8 165. Lemp MA, Dilly PN, Boyde A. Tandem-scanning (confocal) microscopy of the full-
9 thickness cornea. Cornea. 1985-1986;4(4):205-9.
10
11
12
13
14
15
16
17
18
19
20
21
22
23
24
25
26
27
28
29
30
31
32
33
34
35
36
37
38
39
40
41
42
43
44
45
46
47
48
49
50
51
52
53
54
55
56
57
58
59
60

For Peer Review Only

Declaration of interest:

The authors report no conflicts of interest.

The authors alone are responsible for the content and writing of the paper.

Funding

Supported in part by:

Research to Prevent Blindness, New York, New York (unrestricted departmental grant, and SVP as Olga Keith Wiess Scholar), Mayo Foundation, Rochester, MN, NIH Grant EY11915 (SCP), an unrestricted grant from Research to Prevent Blindness, New York, NY (SCP), the Oshman Foundation, Houston, TX (SCP), the William Stamps Farish Fund, Houston, TX (SCP), Hamill Foundation, Houston, TX (SCP)

Figure Legends

Figure 1. Laser IVCN appearance of Acanthamoeba cysts demonstrating clustering of cysts (A), Acanthamoeba cysts demonstrating linear alignment of cysts (B), and Acanthamoeba trophozoites (C, D).

Figure 2. Laser ICVM appearance of Fusarium Solani hyphae (A), Paecilomyces Lilacinus hyphae (B), and Candida Parapsilosis (C).

Figure 3. Representative confocal microscopy of meibomian glands scans of normal control subject (A), meibomian gland dysfunction (MGD) patients (B), and Sjogren Syndrome (SS) patient (C). Please note the decreased density and the enlargement of acinar unit and the increased secretion reflectivity in MGD patient (B). SS patient shows small acinar units, with increased density of inflammatory cells and increased inhomogeneity of the periglandular interstice (C).

Figure 4. Representative impression cytology imprint and confocal microscopy scans of bulbar conjunctiva in normal control subject (A, C) and Sjogren syndrome patient (B, D). The squamous metaplasia was observed both in impression cytology and confocal microscopy examination.

Figure 5. IVCN appearance of microcysts of aqueous humor in the conjunctival epithelium over a filtering bleb after trabeculectomy

Figure 6. Corneal epithelial changes in glaucoma patient, showing anisocytosis and inflammatory cells.

Figure 7. Extensive formation of microdots in the corneal stroma of a rigid lens wearer.

Figure 8. IVCN appearance of microcysts in the bulbar conjunctiva of an asymptomatic soft contact lens wearer.

Figure 9. Real-time mapping of SNP structures (A) and results of automatic quantification of SNP structures using in house developed software (B).

1
2
3
4
5
6
7
8
9
10
11
12
13
14
15
16
17
18
19
20
21
22
23
24
25
26
27
28
29
30
31
32
33
34
35
36
37
38
39
40
41
42
43
44
45
46
47
48
49
50
51
52
53
54
55
56
57
58
59
60

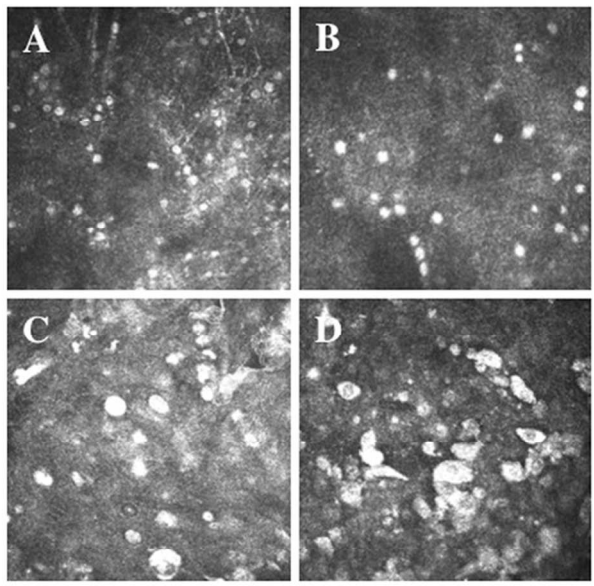


Figure 1. Laser IVCM appearance of Acanthamoeba cysts demonstrating clustering of cysts (A), Acanthamoeba cysts demonstrating linear alignment of cysts (B), and Acanthamoeba trophozoites C, D). 169x127mm (150 x 150 DPI)

Review Only

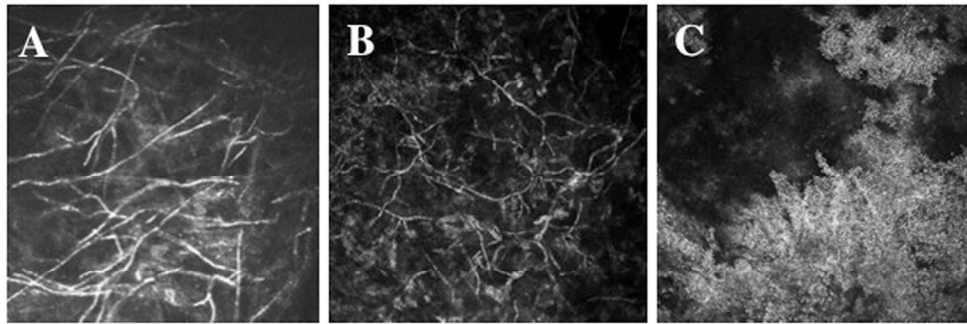


Figure 2. Laser ICVM appearance of *Fusarium Solani* hyphae (A), *Paecilomyces Lilacinus* hyphae (B), and *Candida Parapsilosis* (C).
203x77mm (150 x 150 DPI)

Peer Review Only

1
2
3
4
5
6
7
8
9
10
11
12
13
14
15
16
17
18
19
20
21
22
23
24
25
26
27
28
29
30
31
32
33
34
35
36
37
38
39
40
41
42
43
44
45
46
47
48
49
50
51
52
53
54
55
56
57
58
59
60

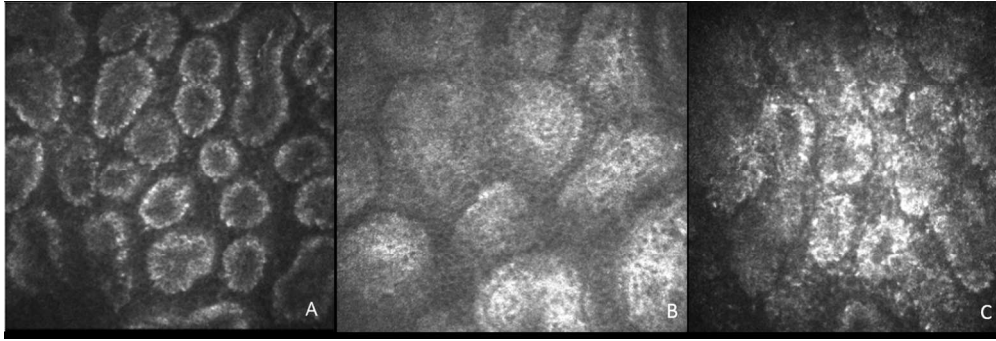
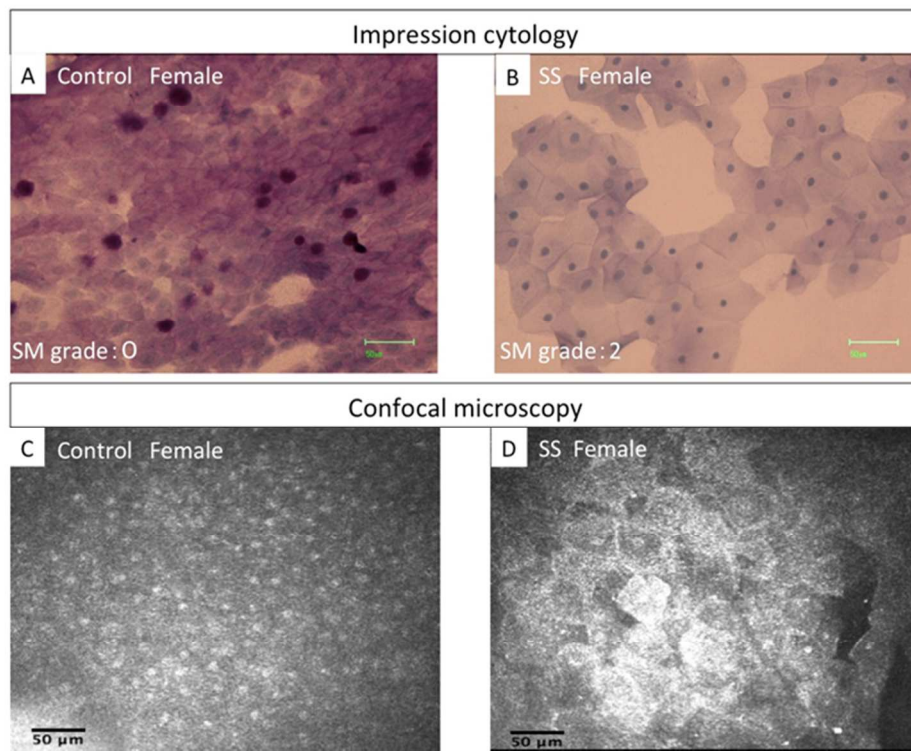


Figure 3. Representative confocal microscopy of meibomian glands scans of normal control subject (A), meibomian gland dysfunction (MGD) patients (B), and Sjogren Syndrome (SS) patient (C). Please note the decreased density and the enlargement of acinar unit and the increased secretion reflectivity in MGD patient (B). SS patient shows small acinar units, with increased density of inflammatory cells and increased inhomogeneity of the periglandular interstice (C).

290x97mm (150 x 150 DPI)



32 Figure 4. Representative impression cytology imprint and confocal microscopy scans of bulbar conjunctiva
33 in normal control subject (A, C) and Sjogren syndrome patient (B, D). The squamous metaplasia was
34 observed both in impression cytology and confocal microscopy examination.
35 149x112mm (150 x 150 DPI)

36
37
38
39
40
41
42
43
44
45
46
47
48
49
50
51
52
53
54
55
56
57
58
59
60

1
2
3
4
5
6
7
8
9
10
11
12
13
14
15
16
17
18
19
20
21
22
23
24
25
26
27
28
29
30
31
32
33
34
35
36
37
38
39
40
41
42
43
44
45
46
47
48
49
50
51
52
53
54
55
56
57
58
59
60

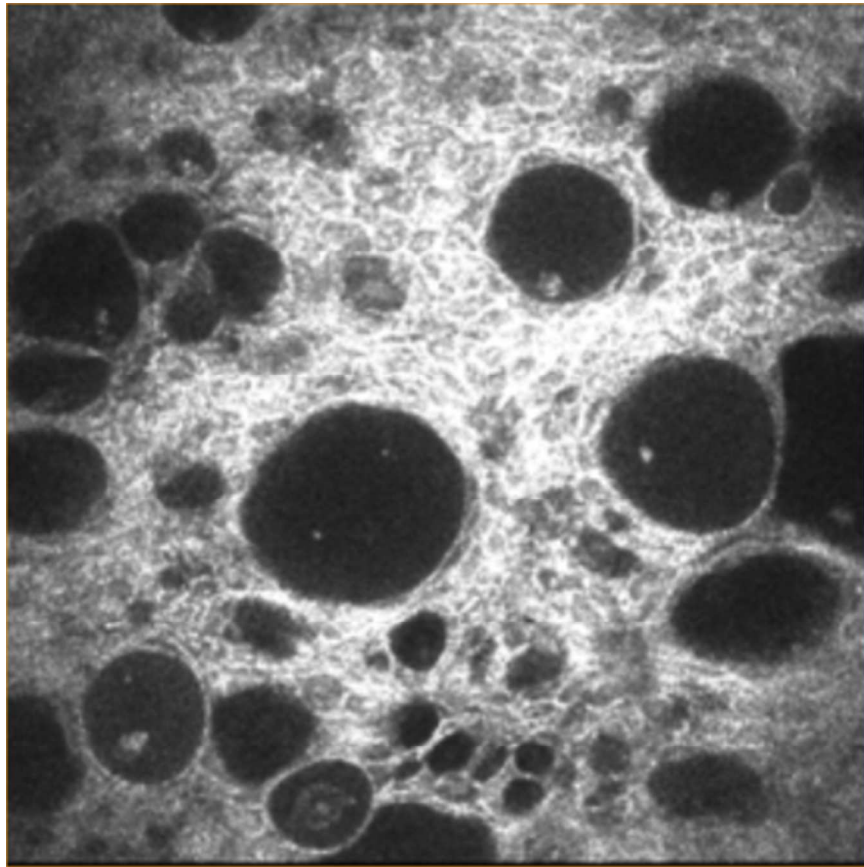


Figure 5. IVCM appearance of microcysts of aqueous humor in the conjunctival epithelium over a filtering bleb after trabeculectomy
73x73mm (150 x 150 DPI)

Only

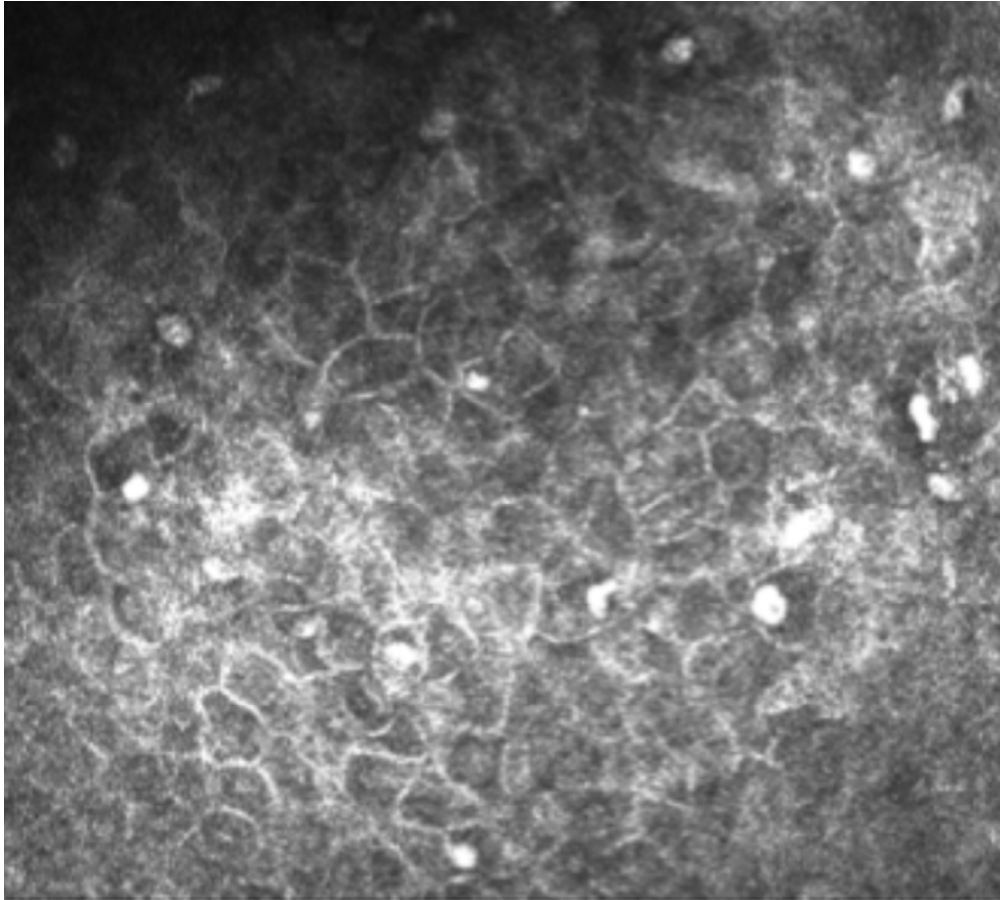
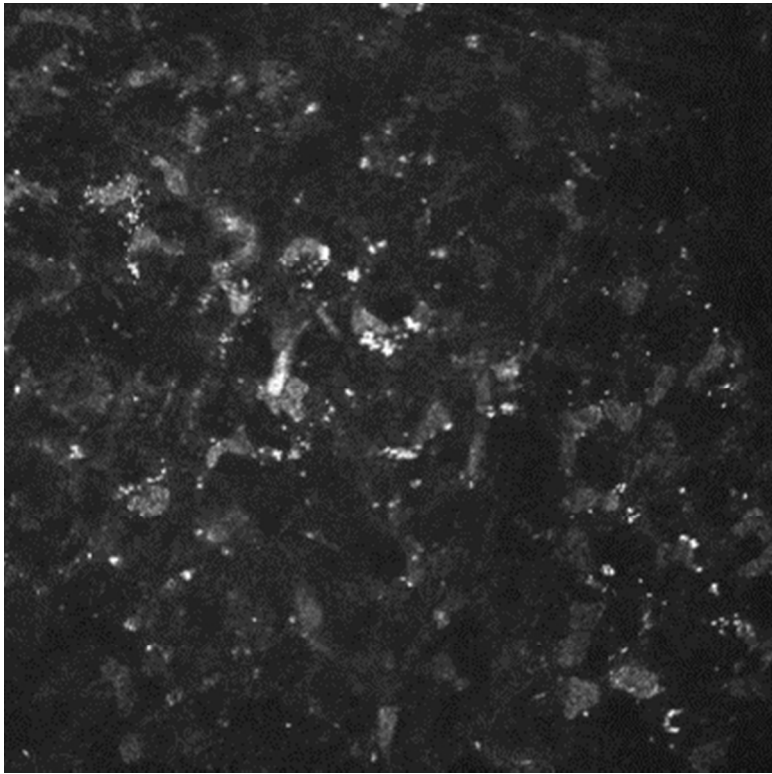


Figure 6. Corneal epithelial changes in glaucoma patient, showing anisocytosis and inflammatory cells.
130x117mm (150 x 150 DPI)

Only

1
2
3
4
5
6
7
8
9
10
11
12
13
14
15
16
17
18
19
20
21
22
23
24
25
26
27
28
29
30
31
32
33
34
35
36
37
38
39
40
41
42
43
44
45
46
47
48
49
50
51
52
53
54
55
56
57
58
59
60



Extensive formation of microdots in the corneal stroma of a rigid lens wearer.
101x101mm (96 x 96 DPI)

View Only

1
2
3
4
5
6
7
8
9
10
11
12
13
14
15
16
17
18
19
20
21
22
23
24
25
26
27
28
29
30
31
32
33
34
35
36
37
38
39
40
41
42
43
44
45
46
47
48
49
50
51
52
53
54
55
56
57
58
59
60

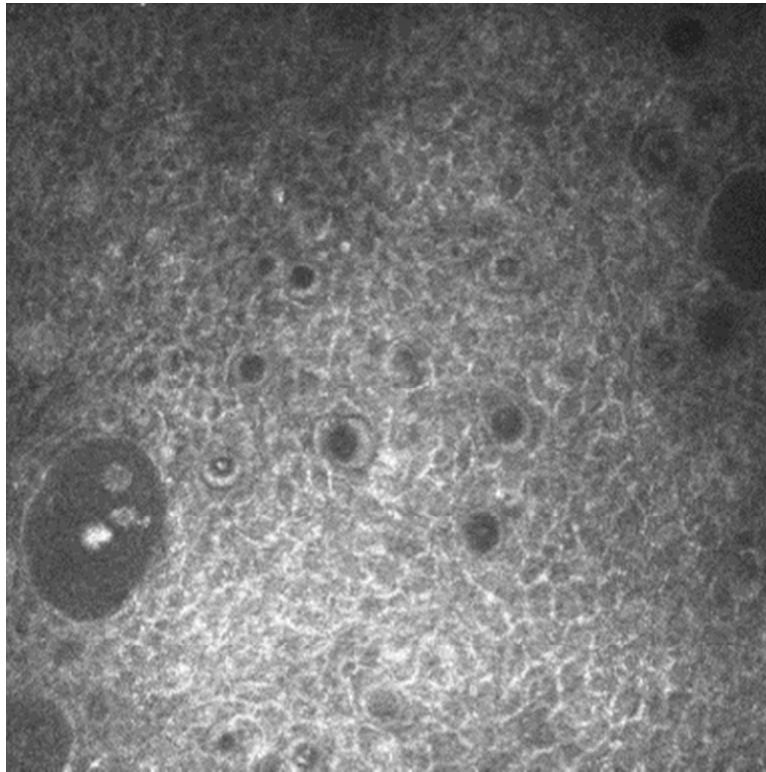


Figure 8. IVCM appearance of microcysts in the bulbar conjunctiva of an asymptomatic soft contact lens wearer.
101x101mm (96 x 96 DPI)

ew Only

1
2
3
4
5
6
7
8
9
10
11
12
13
14
15
16
17
18
19
20
21
22
23
24
25
26
27
28
29
30
31
32
33
34
35
36
37
38
39
40
41
42
43
44
45
46
47
48
49
50
51
52
53
54
55
56
57
58
59
60

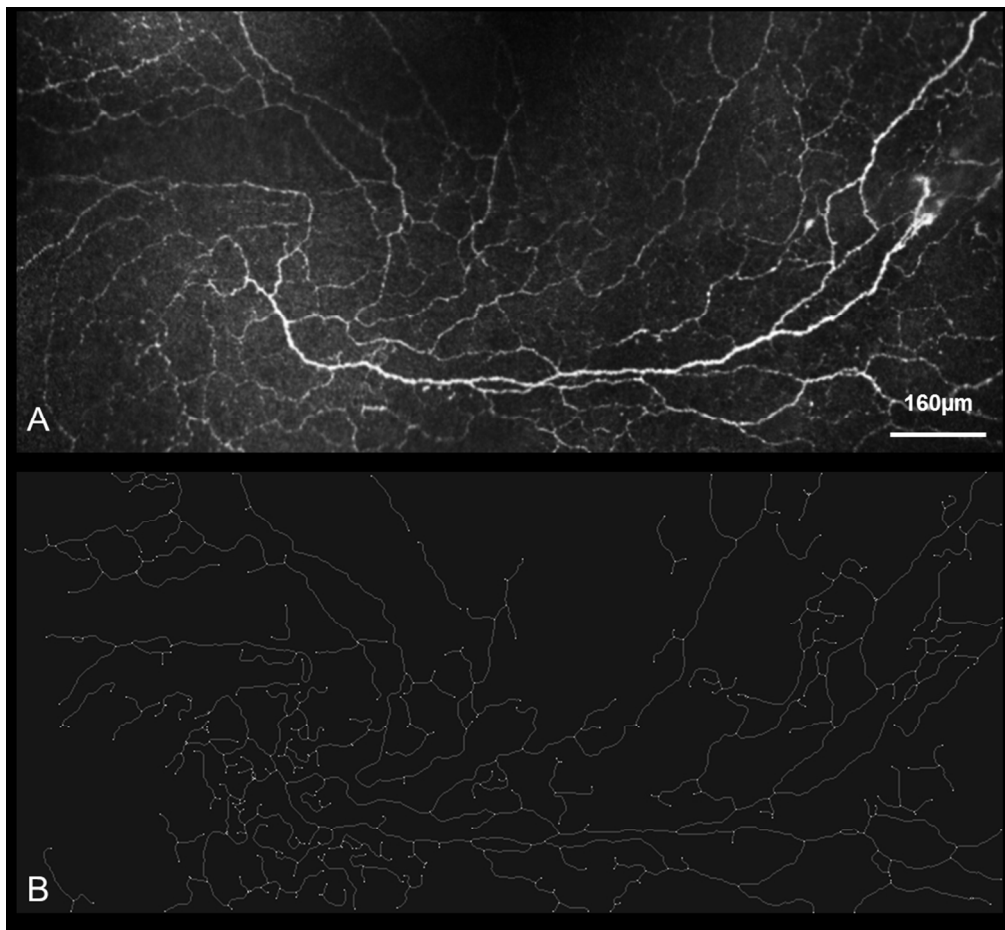


Figure 9. Real-time mapping of SNP structures (A) and results of automatic quantification of SNP structures using in house developed software (B).
187x172mm (150 x 150 DPI)

Only